Interstellar extinction and the problem of cosmic abundances

Nikolai Voshchinnikov

Sobolev Astronomical Institute
St. Petersburg University

Interstellar medium (ISM)

Main components: ***gas and dust***

Location: ***IS clouds (diffuse, dense, translucent)***

Main problem: ***determination of the chemical composition of the ISM + study of the chemical evolution of Galaxy (galaxies)***

IS gas

Observational manifestations:

absorption lines and bands (clouds); emission lines (HII regions, hot gas)

IS dust

Observational manifestations:

IS extinction and polarization (clouds); e scattered radiation (nebulae, circumstellar shells); IR radiation (continuum + bands; clouds, nebulae, CS shells,…)

IS gas + dust = cosmic abundance

$$[X/H]_g + [X/H]_d = [X/H]_{cosmic}$$

5 elements: C, O, Mg, Si, Fe

Gas: absorption lines

Dust: IS extinction curves

Abundances:

Reference, cosmic, interstellar, solar

COSMIC → Sun

$$\left[\frac{X}{H}\right]_d = \left[\frac{X}{H}\right]_{cosmic} - \left[\frac{X}{H}\right]_g$$

Interstellar dust grains consist of five the most «important» elements:

Units:

ppm – parts per million

N(X)/N(H)*10^6

K, Ti, Cr, Mn, Co – traces (less than 0.3 ppm)

Abundances

	old solar (1989)	new solar (2004)	stellar (1996)	zeta Oph (dust)
C	363	245	214	110
O	851	457	457	126
Mg	38.0	33.9	25	31.9
Si	35.5	34.2	18.6	32.6
Fe	32.4	28.2	27	28.2

1996, Snow & Witt:

C /H(Sun) – 363 ppm

C /H(stars) – 214 ppm

~150 ppm!

has been taken from the solid phase

Result: CARBON CRISIS

«Time variations» of carbon and oxygen abundances in the solar atmosphere

Table 1: C, N, O abundances as implied from a variety of different atomic and molecular indica
using a 3D hydrodynamical model of the solar atmosphere (Asplund et al. 2005a). Results from
semi-empirical 1D model of Holweger-Müller (1974) are given for comparison. The last column gives
difference between 3D- and 1D-based results

Lines	CNO abundances		
	3D	HM	3D-1D
[CI]	8.39	8.45	-0.06
CI	8.36 ± 0.03	8.39 ± 0.03	-0.03
CH Δv=1	8.38 ± 0.04	8.53 ± 0.04	0.15
C_2 Swan	8.44 ± 0.03	8.53 ± 0.03	-0.09
CH A-X	8.45 ± 0.04	8.59 ± 0.04	-0.14
CO Δv=1	8.41 ± 0.02	8.62 ± 0.02	-0.21
CO Δv=2	8.38 ± 0.02	8.70 ± 0.03	-0.32
NI	7.85 ± 0.08	7.97 ± 0.08	-0.12
NH Δv=1	7.73 ± 0.05	7.95 ± 0.05	-0.22
[OI]	8.68 ± 0.01	8.76 ± 0.02	-0.08
OI	8.64 ± 0.02	8.64 ± 0.08	0.00
OH Δv=0	8.61 ± 0.03	8.82 ± 0.01	-0.21
OH Δv=1	8.61 ± 0.03	8.87 ± 0.03	-0.26

261ppm

IS dust composition

***C* – amorphous carbon, graphite**

***O* – oxides (FeO, Fe_2O_3, Fe_3O_4, MgO, SiO, H_2O)**

***Si* – silicates (olivines, pyroxenes)**

***Mg* – silicates, oxide**

***Fe* – pure iron, silicates, oxides**

10мкм полоса: растяжение связи Si - O

Olivines

(оливково-зеленый цвет)

$Mg_{2x}Fe_{2-2x}SiO_4$, $0<=x<=1$

x=1: Mg_2SiO_4 - forsterite (A.J. Forster – английский коллекционер минералов и торговец)

x=0: Fe_2SiO_4- fayalite (место находки о. Фаял, Азорские о-ва)

Pyroxenes

(от греч. «огонь» + «чужеземец»)

$Mg_xFe_{1-1x}SiO_3$, $0<=x<=1$

x=1: $MgSiO_3$ - enstatite (от греч. «противник», трудно плавится)

x=0: $FeSiO_3$- ferrosilite (по составу)

Это – твердые растворы внедрения (interstitial solid solutions)

IS gas

IS absorption lines:

equivalent line width W_λ gives

N_X – column density of atom (ion)

$$W_\lambda = 8.85 \times 10^{-21} N f \lambda^2$$

W_λ and λ are in Å and N is in cm^{-2}.

***Method:** curve of growth*

Ions and lines

	E_{ion}, eV	Ions	Lines, A
C	11.3	CI, CII	2325, …
O	13.6	OI	1356, …
Mg	7.65	MgII	1026, 1240, …
Si	8.1	SiII	2235,…
Fe	7.87	FeII	1055, 1143, 2249, 2267

Results

Dependencies $N(X)/N(H)$

on D – distance to the star

$\langle n(H) \rangle = N(H)/D$ - mean concentration of H

$f(H_2)$ – fraction of H_2 on the line of sight

E(B-V) – colour excess

……

Miller et al. ApJ 659, 441, 2007 (STIS+FUSE)

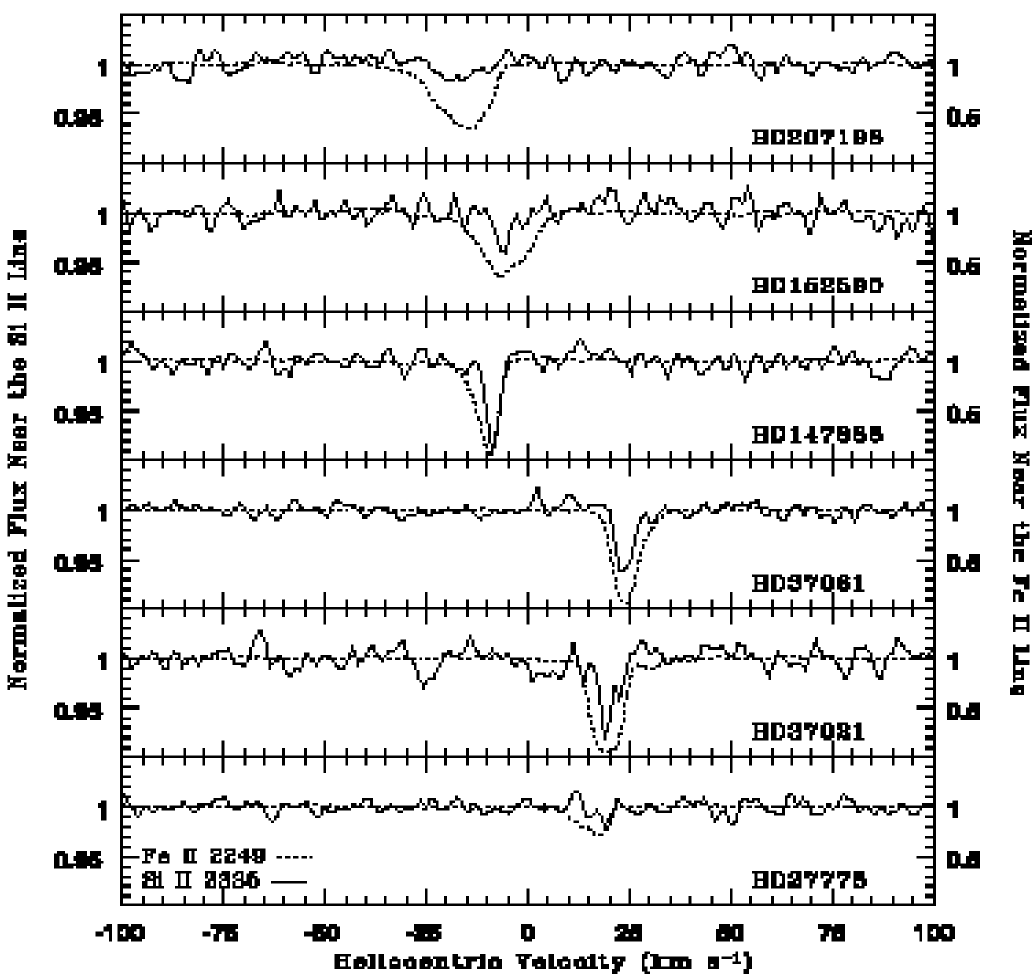

FIG. 1. Normalized STIS echelle spectra of the Si II] λ2335 (*solid line*) and Fe II λ2249 (*dotted line*) absorption features. Note that the normalized flux scale is on the left for silicon and on the right for iron.

Cartledge et al. ApJ 641, 327, 2006 (STIS)

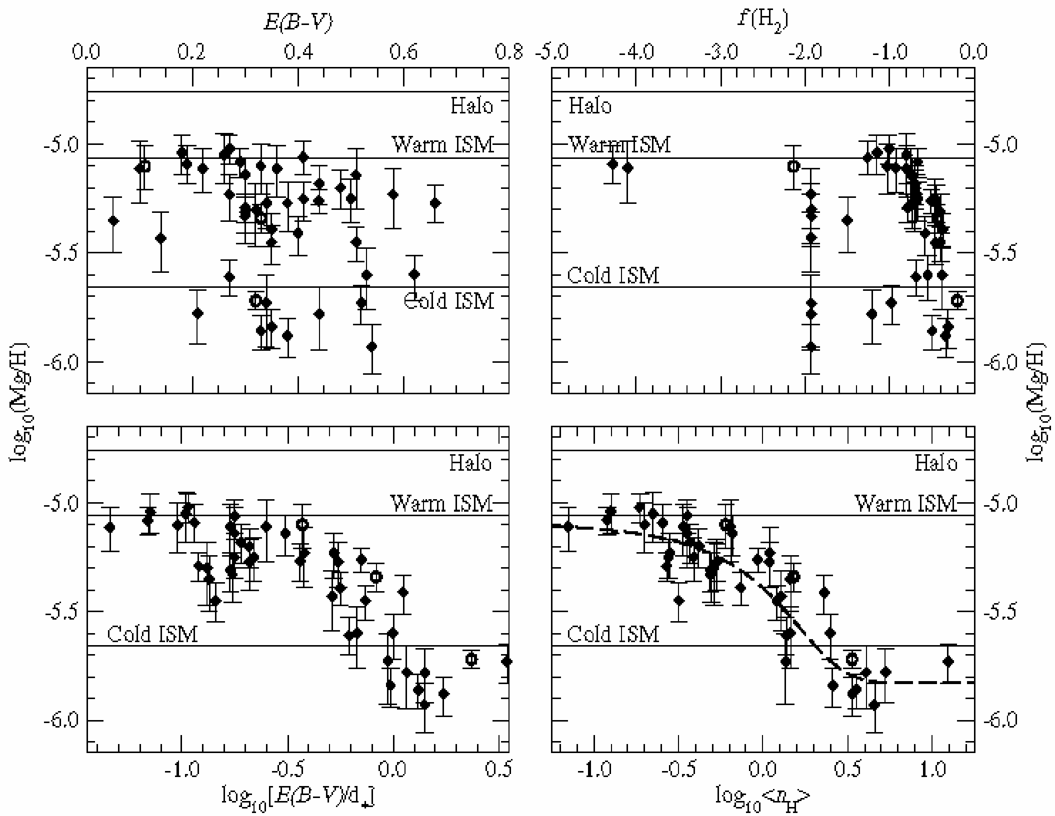

Fig. 9. Magnesium gas-phase abundances expressed relative to $E(B-V)$, $E(B-V)/d_*$, $f(H_2)$, and $\langle n_H \rangle$. Magnesium has been selected to test the gas-phase abundance variations for more heavily depleted elements with sight line properties other than mean hydrogen sight line density. As with germanium, only $E(B-V)/d_*$ approaches the effectiveness of $\langle n_H \rangle$. HD156110 has been omitted from this figure.

Jensen & Snow ApJ 669, 378, 2007 (STIS+FUSE)

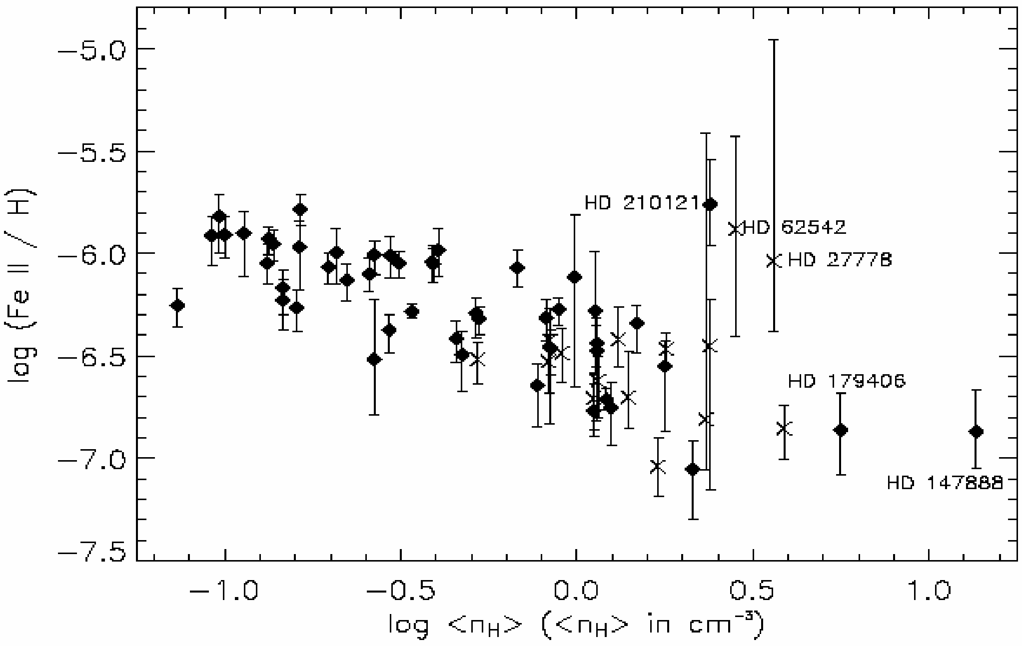

Fig. 6.— The logarithmic abundance of Fe II relative to hydrogen plotted against the logarithm of the average volume density of hydrogen. **Solid diamonds**:—abundances derived in this paper. **X's**:—abundances based on column densities derived in SRF2002. The three lines of sight that do not follow the general trend of increased depletion with increased average volume density of hydrogen are HD 210121 from this paper and HD 27778 and HD 62542 from SRF2002. Note that the two densest lines of sight, HD 179406 and HD 147888, follow the trend but do not show significantly enhanced iron depletion.

Jensen & Snow ApJ 669, 401, 2007 (STIS+FUSE)

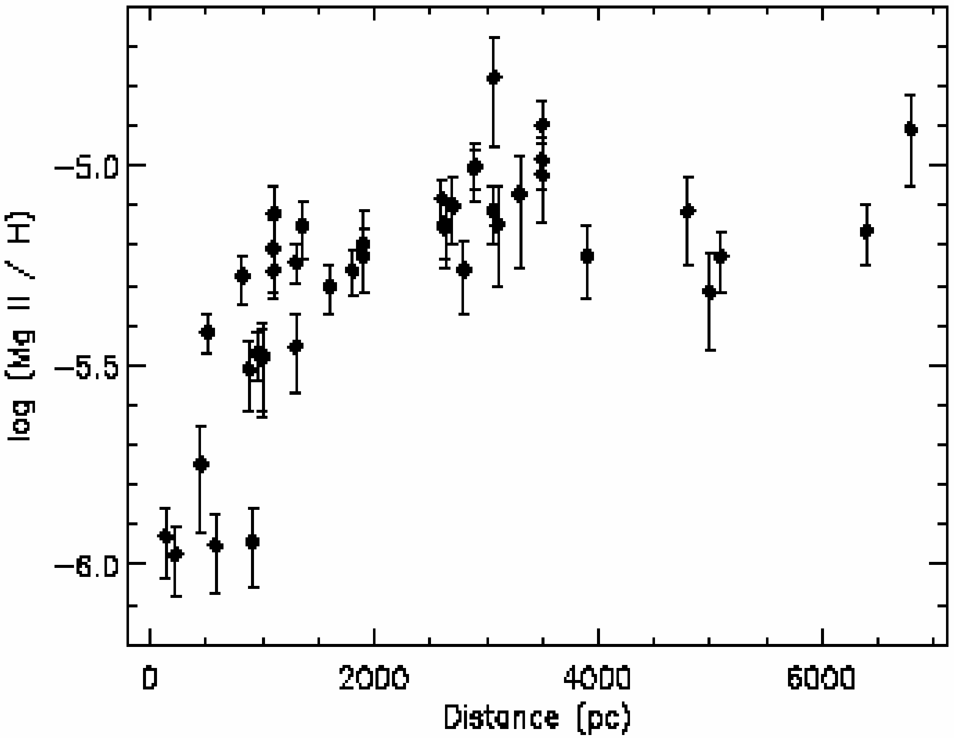

Fig. 7.— The logarithmic abundance of Mg II relative to hydrogen plotted against path length. Note the trend of decreasing depletion up to about 1.5-2 kpc, and relatively constant depletion beyond 2 kpc.

Recent results

Data: ***(gas-phase abundances)***

O: ***Cartledge...2001 ApJ 562, 394 (11 stars)***
Jensen,....2005 ApJ 619, 891 (26 stars; 10 HST)
Cartledge...2004 ApJ 613, 1037 (36/ stars)
Meyer...1998 ApJ 493, 222 (7 stars)
Andre...2003 ApJ 591, 1000 (19 stars)

Mg: ***Jensen, Snow, 2007 (44 stars)***
Cartledge,... ApJ 641, 327, 2006 (47 stars)

Fe: ***Miller,2007 ApJ 659, 441 (6 stars)***
Jensen, Snow, 2007 (51 stars)
Snow et al., ApJ 573, 662, 2002 (18 stars)

+ D, E(B-V), A(V), R(V)=A(V)/E(B-V),…

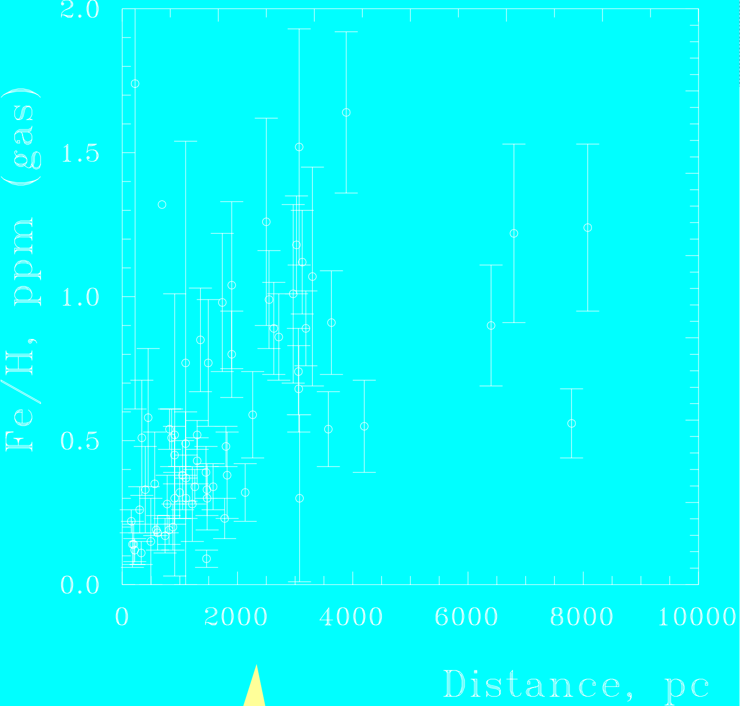

70 stars

77 stars

88 stars

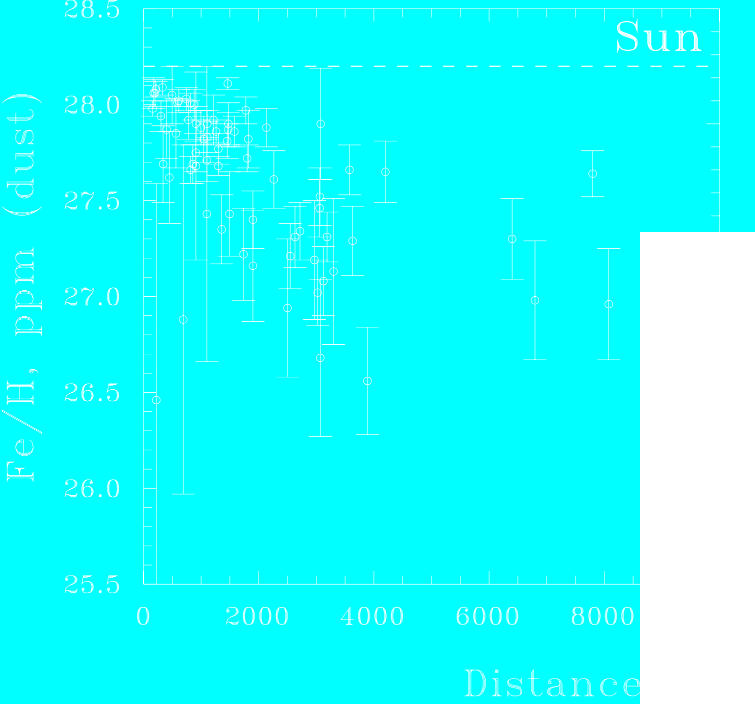

[Fe/H]$_{Sun}$=28.2ppm

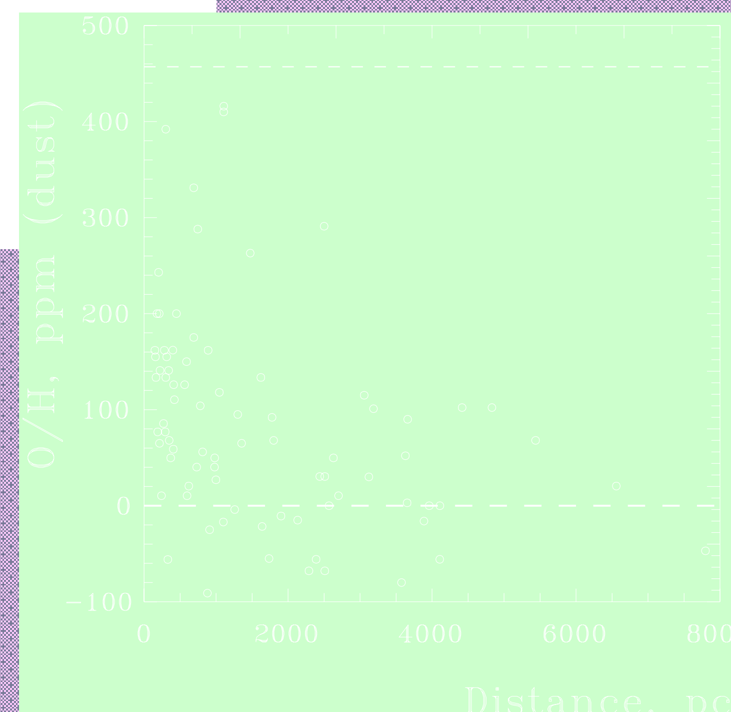

[Mg/H]$_{Sun}$=33.9ppm

[O/H]$_{Sun}$=457ppm

Some conclusions

Dust-phase abundance of Mg and Fe (?) decreases with growth of distance to the star

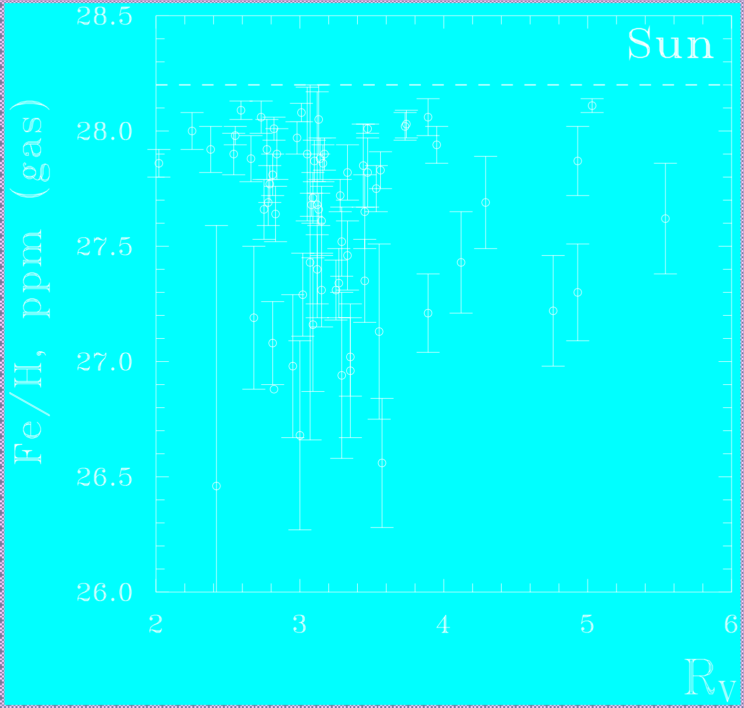
Sun
Fe/H, ppm (gas)
R_V
28.5
28.0
27.5
27.0
26.5
26.0
2
3
4
5
6

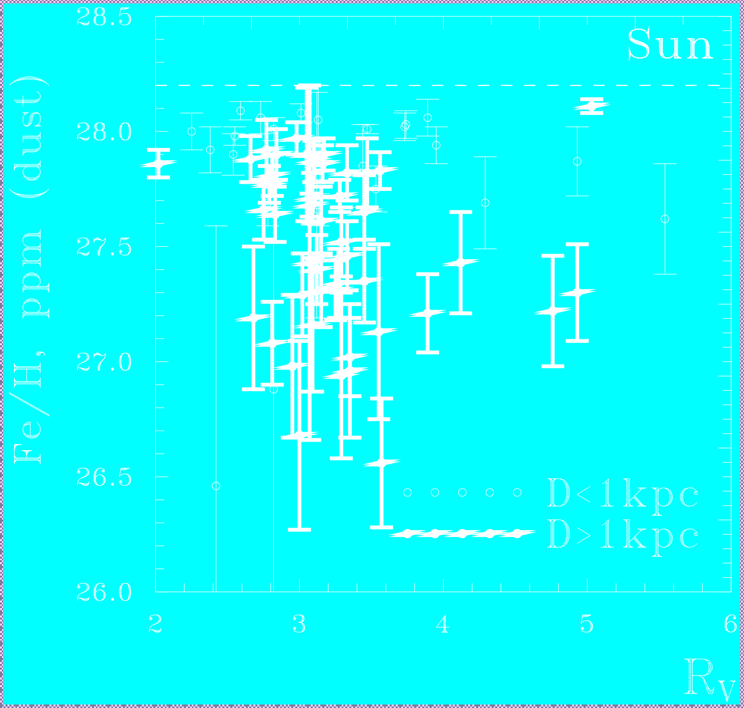
Sun
Fe/H, ppm (dust)
D<1kpc
D>1kpc
R_V
28.5
28.0
27.5
27.0
26.5
26.0
2
3
4
5
6

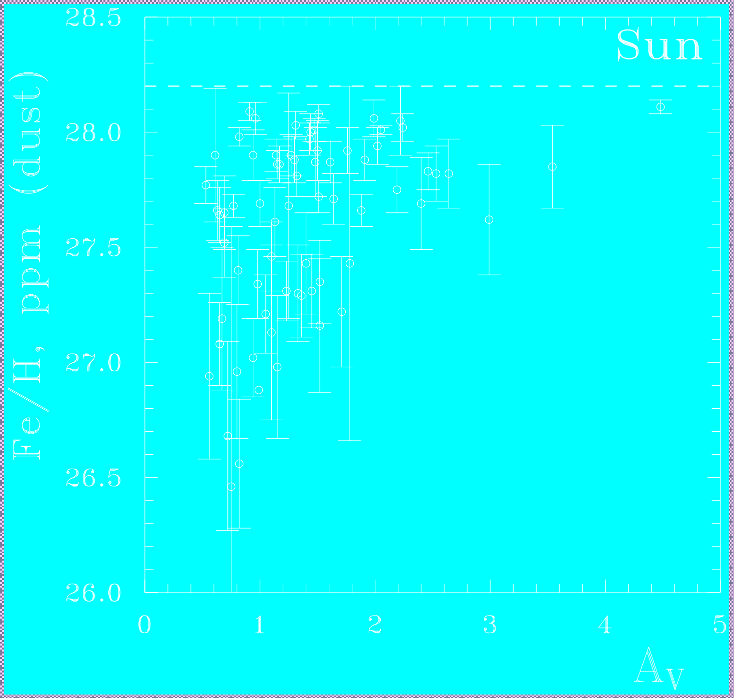
Sun
Fe/H, ppm (dust)
28.5
28.0
27.5
27.0
26.5
26.0
0
1
2
3
4
5
A_V

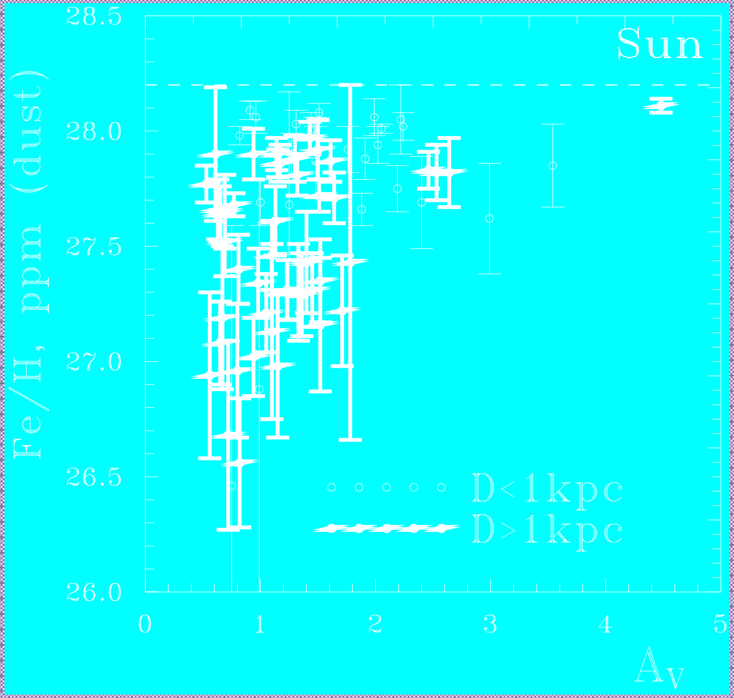
Sun
Fe/H, ppm (dust)
28.5
28.0
27.5
27.0
26.5
26.0
0
1
2
3
4
5
D<1kpc
D>1kpc
A_V

Stars in Orion and rho Oph cloud

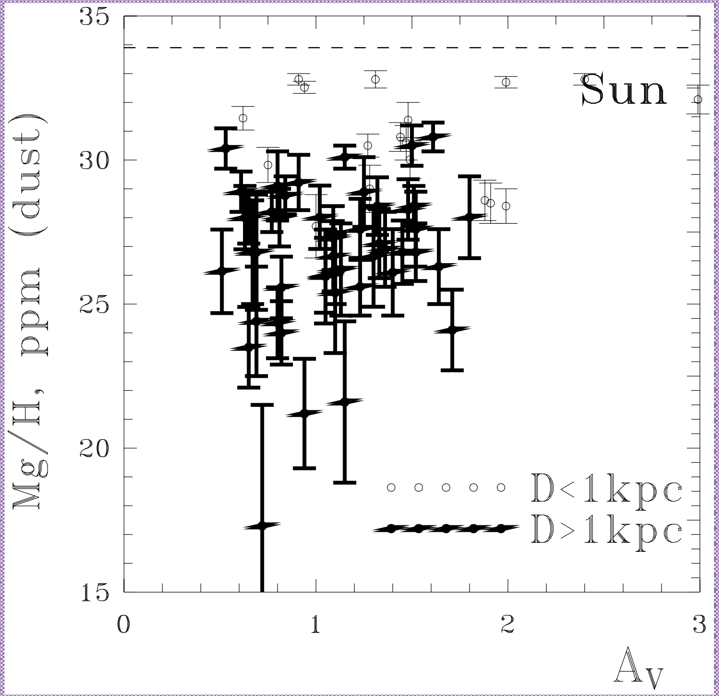

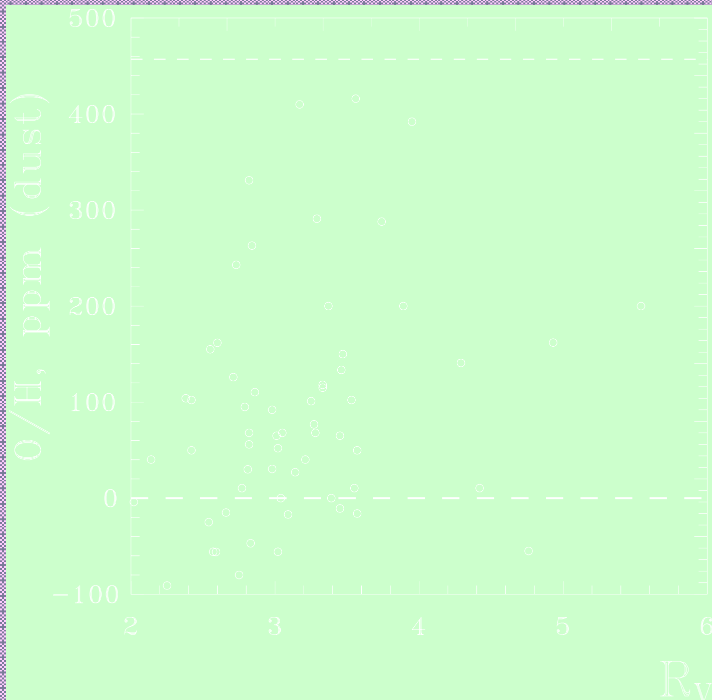
O/H, ppm (dust)
R_V

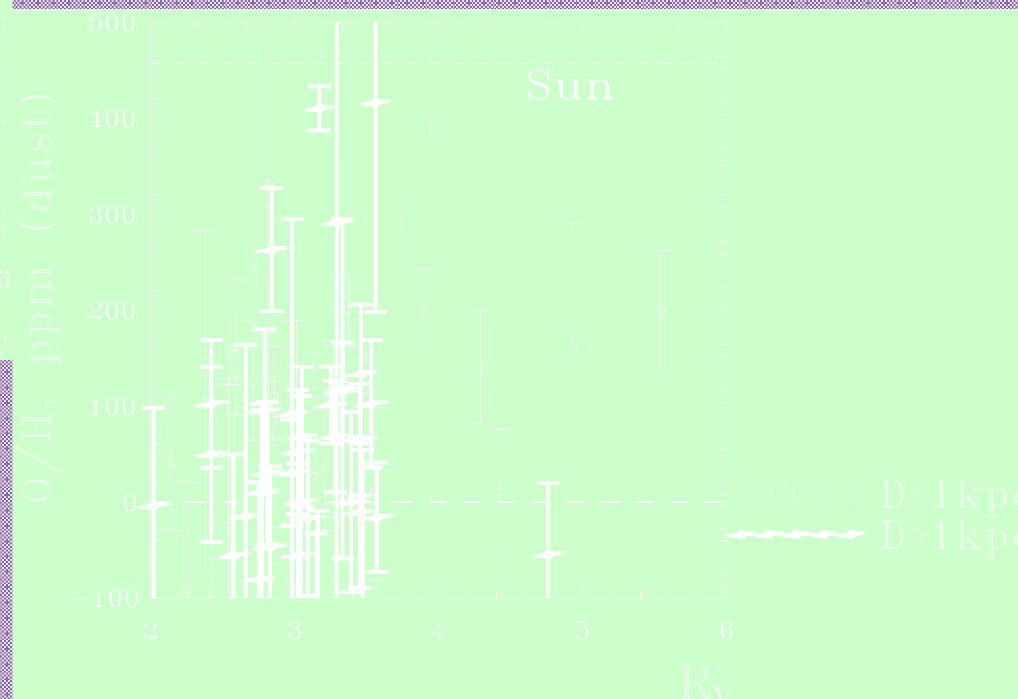
Sun
O/H, ppm (dust)
D<1kpc
D>1kpc
R_V

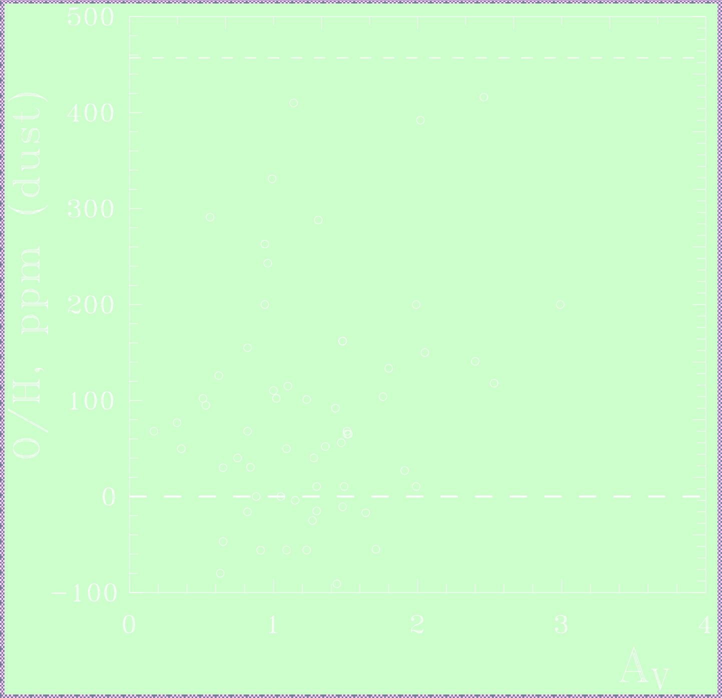

O/H, ppm (dust)
A_V

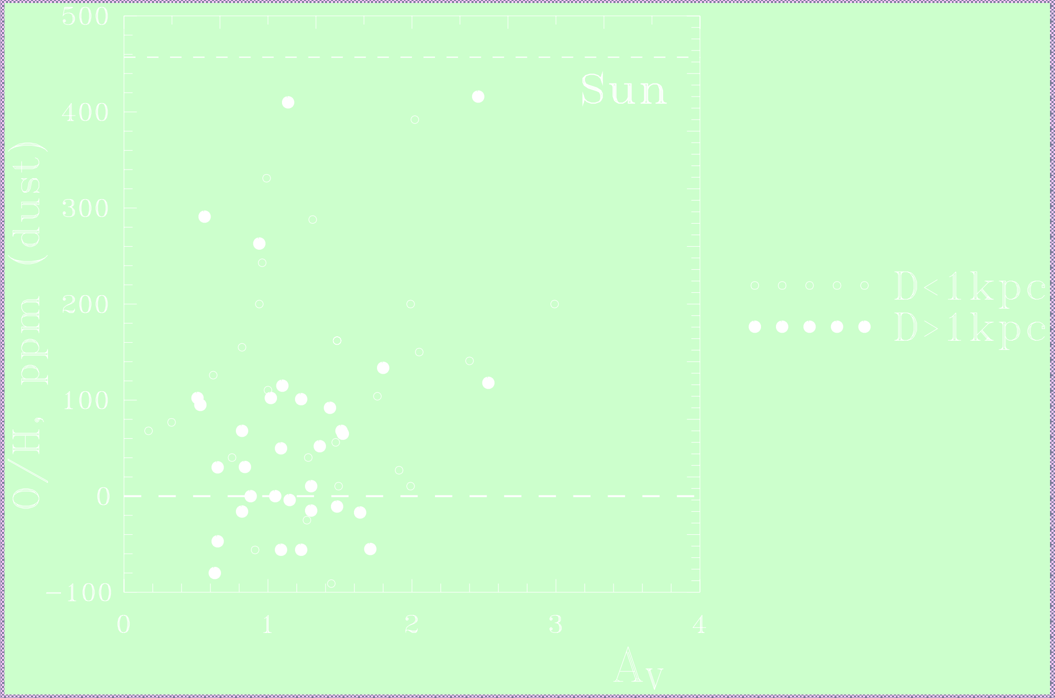

Sun
O/H, ppm (dust)
A_V
D<1kpc
D>1kpc

Some conclusions

It seems there is no correlation of dust-phase abundances of Mg, Fe and O with R(V) and A(V)

Mg/H, ppm (gas)
Fe/H, ppm (gas)

Fe/H, ppm (dust)
Mg/H,

Sun
$A_V<1.5^m$
$A_V>1.5^m$
Fe/H, ppm (dust)
Mg/H, ppm (dust)

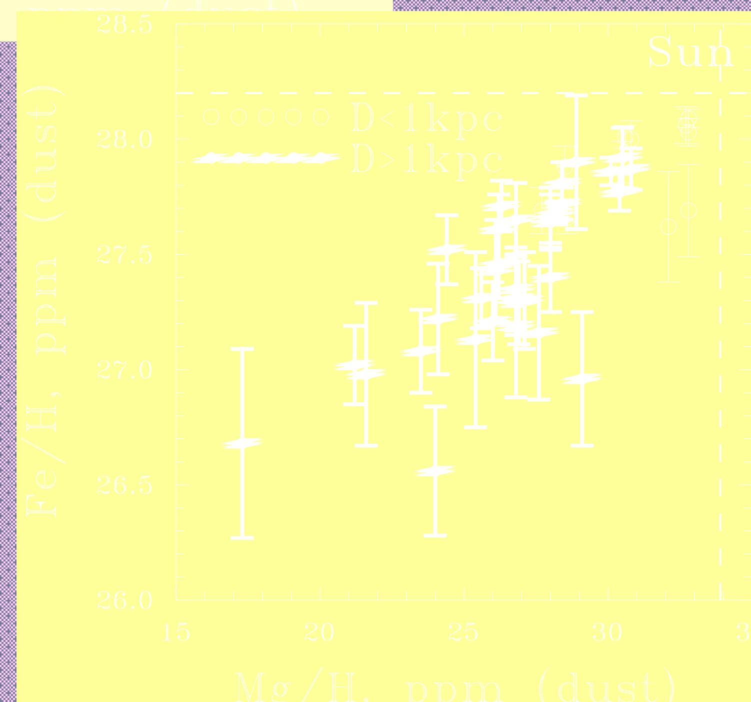
Sun
D<1kpc
D>1kpc
Fe/H, ppm (dust)
Mg/H, ppm (dust)

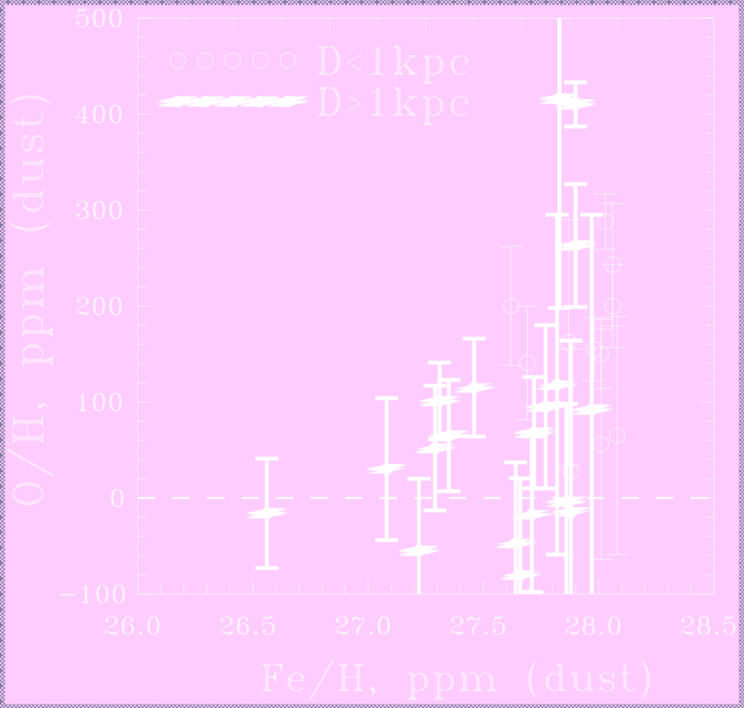
D<1kpc
D>1kpc
O/H, ppm (dust)
Fe/H, ppm (dust)

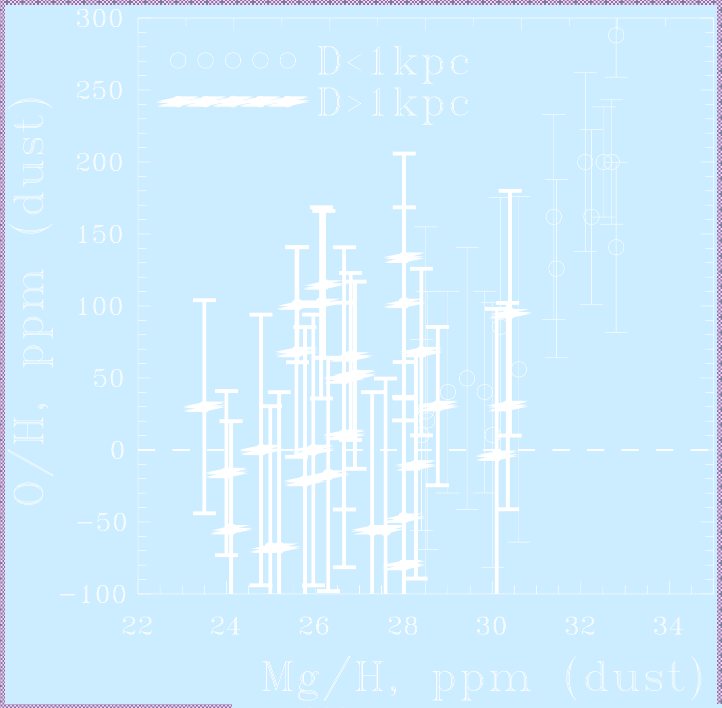
D<1kpc
D>1kpc
O/H, ppm (dust)
Mg/H, ppm (dust)

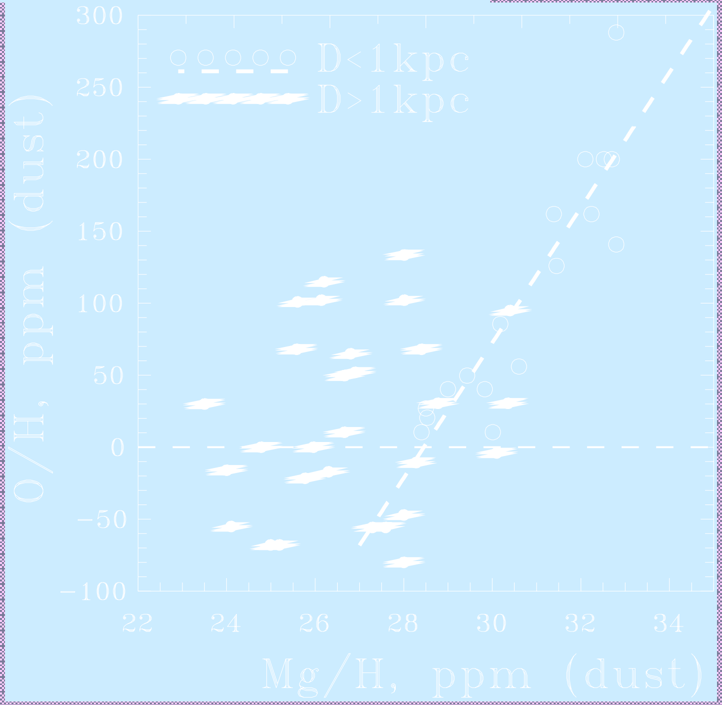
D<1kpc
D>1kpc
O/H, ppm (dust)
Mg/H, ppm (dust)

Some conclusions

It seems there is correlation of dust-phase abundances of Mg-Fe and O-Mg (for not very distant stars)

IS dust

It is possible to determine:

$A(\lambda)$ – interstellar extinction (reddening) curve, usually normalized

$$A^{(n)}(\lambda^{-1}) \equiv \frac{E(\lambda - V)}{E(\mathrm{B} - \mathrm{V})} = \frac{A(\lambda) - A_{\mathrm{V}}}{A_{\mathrm{B}} - A_{\mathrm{V}}} = \frac{\Delta m(\lambda) - \Delta m(V)}{\Delta m(B) - \Delta m(V)}$$

It is possible to estimate: *chemical composition + size of dust grains*

Method: *modelling on the basis of the light scattering theory*

$$\sigma(\lambda) = 4.19 \times 10^{-22} \left(A(\lambda) / A(V) \right)$$

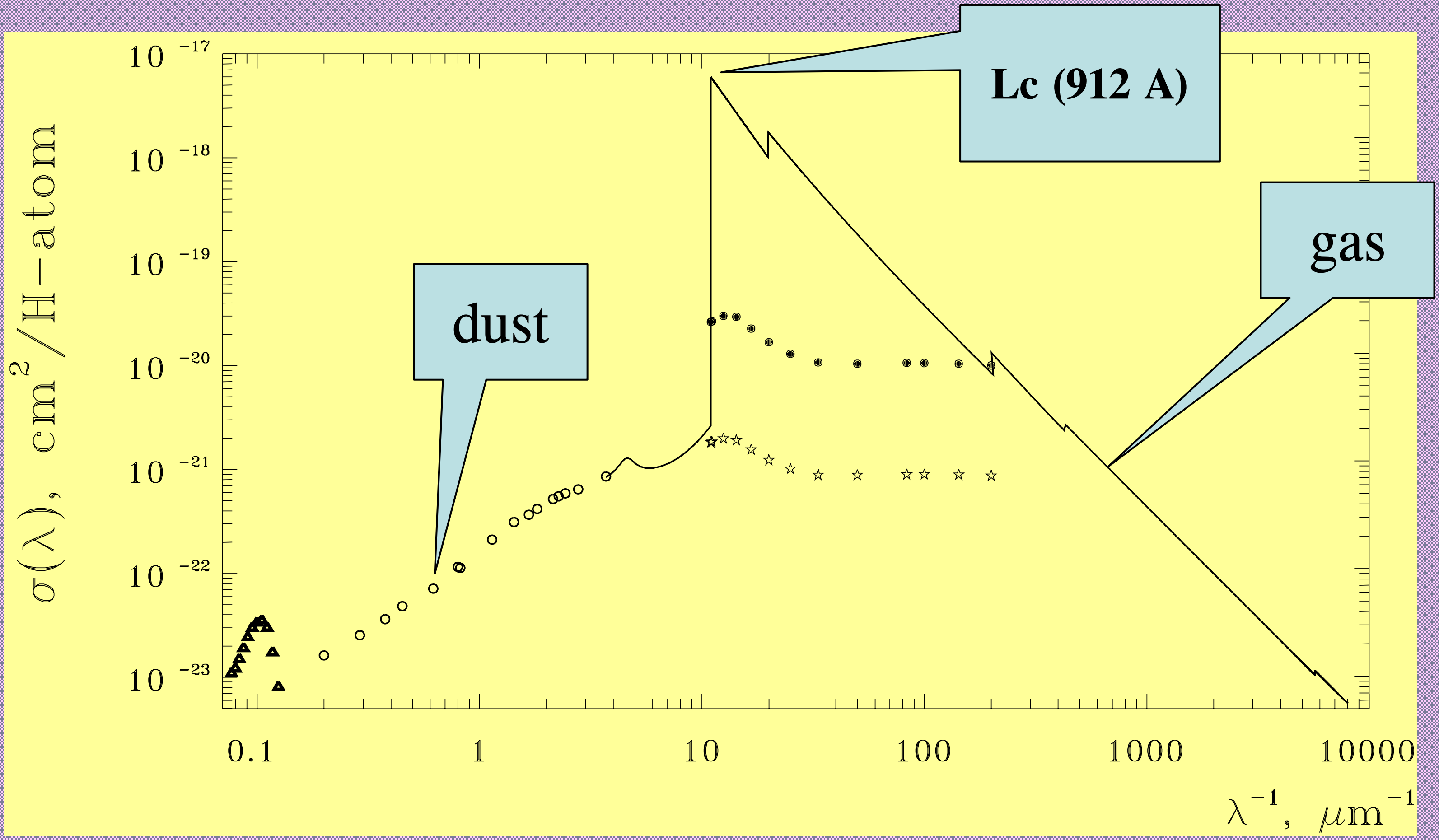

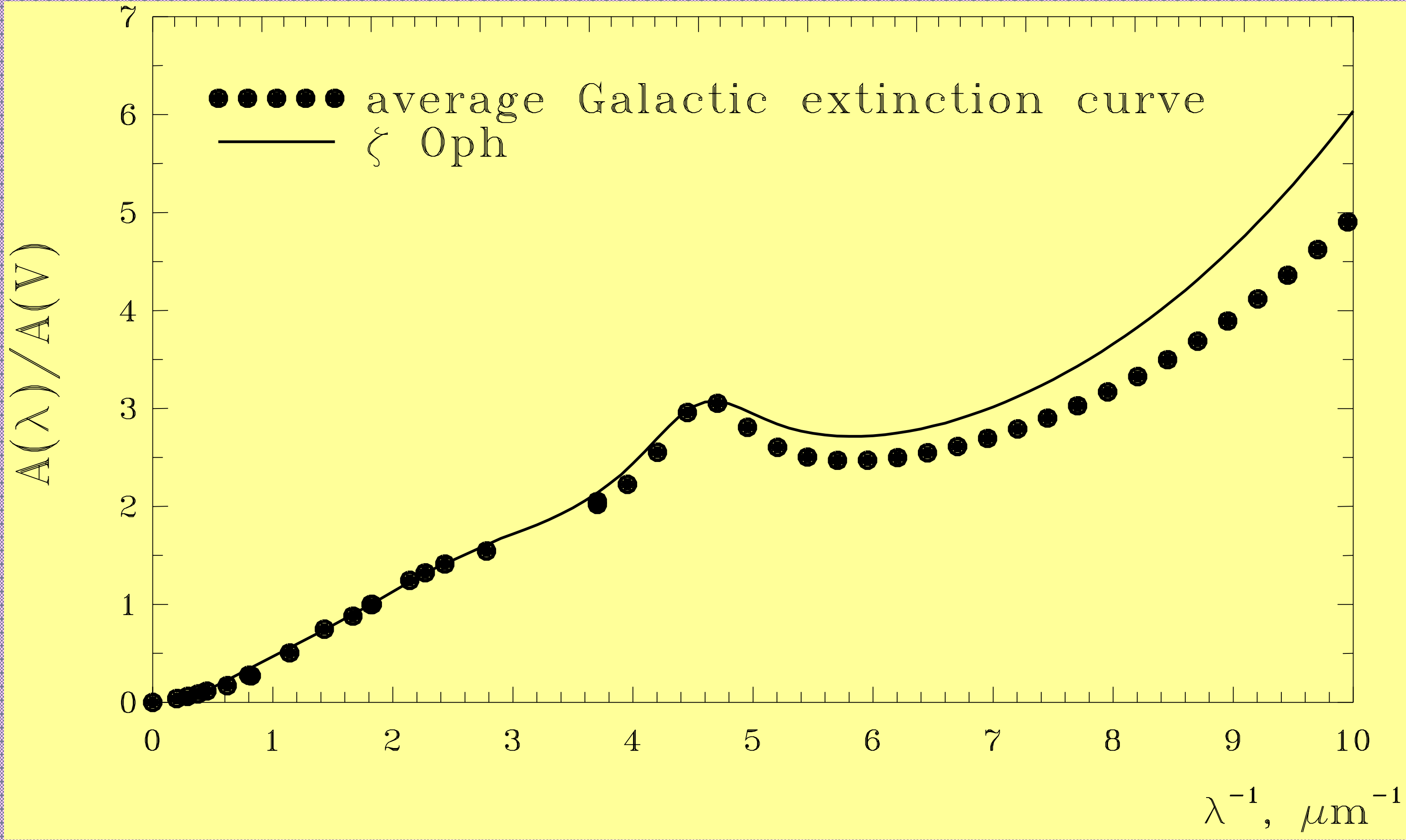

average Galactic extinction curve
ζ Oph
$A(\lambda)/A(V)$
λ^{-1}, μm^{-1}
0
1
2
3
4
5
6
7
8
9
10

UV extinction

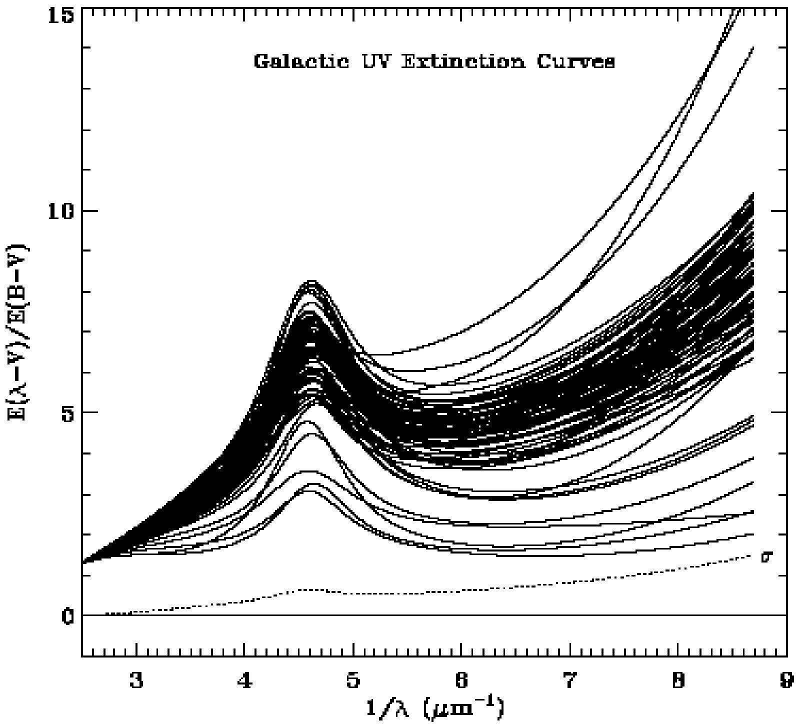

Figure 14 UV extinction curves for 80 galactic stars derived from International Ultraviolet Explorer (IUE) satellite observations. The observational data were fitted using the analytical expressions derived by Fitzpatrick and Massa (1990). After Fitzpatrick (1999).

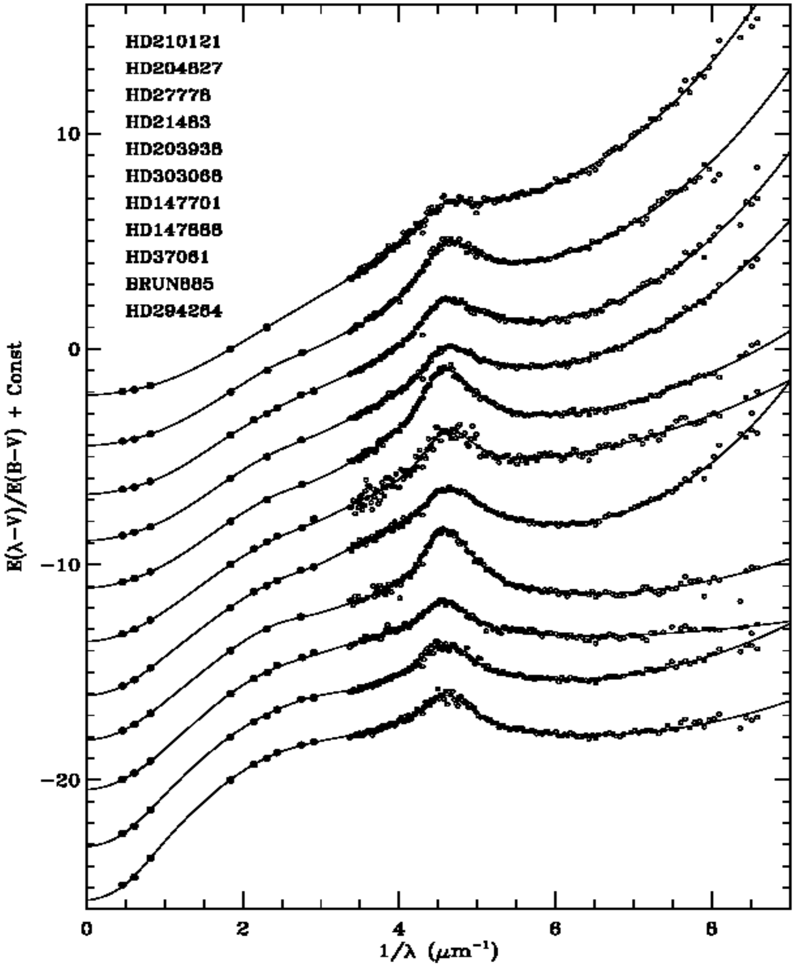

Figure 5. Examples of extinction curves produced with the SED fitting procedure. The smooth curves are the analytical representations of the extinction, which are determined by the fits. The data points show the actual ratios between the reddened star SEDs and the model atmosphere calculations. The curves have been successively offset downwards by 2 units for clarity. The data point at V ($1/\lambda = 1.83\ \mu\mathrm{m}^{-1}$) should be located at $E(\lambda - V)/E(B - V) = 0$ for each curve.

LMC/SMC dust?

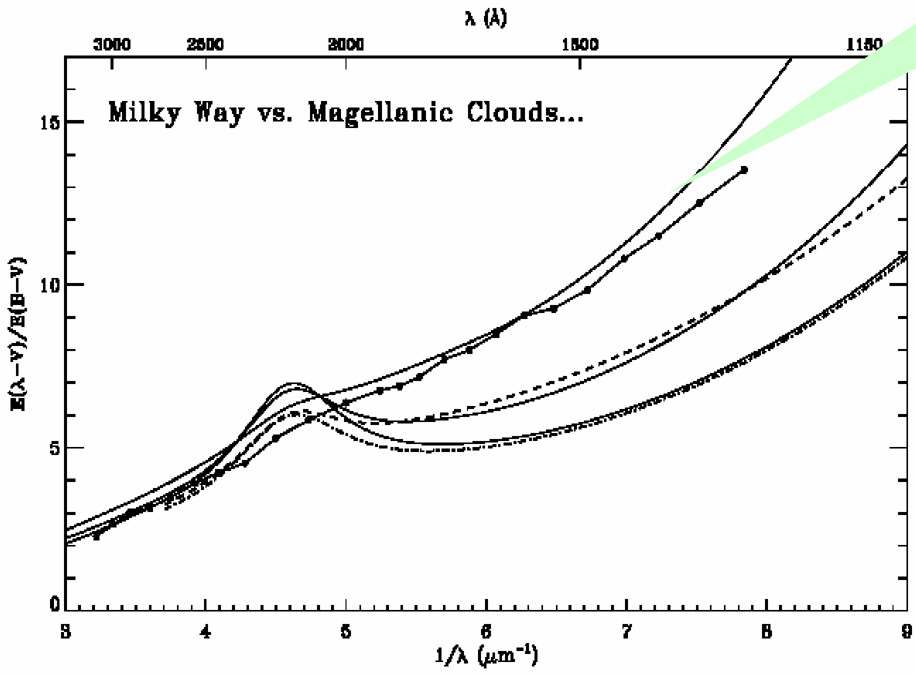

Figure 14. A comparison between idealized Galactic extinction curves with $R = 1.9$, 2.5, and 2.85 and the SMC curve from Prévot et al. (1984; filled circles), the 30 Doradus curve (dashed curve), and the mean LMC curve (dash-dotted curve), respectively. The latter two curves are from Fitzpatrick (1986), as parametrized by Fitzpatrick & Massa (1990).

NO!

Scattered radiation!

Kruegel, 2008

Interpretation

Interstellar extinction:

$$A(\lambda) \approx 1.086\,\tau_{\rm ext}(\lambda) = 1.086\,C_{\rm ext}(\text{composition, size, }\lambda)\,N_{\rm d} =$$

$$1.086\,G\,Q_{\rm ext}(\text{composition, size, }\lambda)\,n_{\rm d}\,D$$

$C_{\rm ext}$(composition, size, λ) – extinction cross-section
$N_{\rm d}$ – column density of dust grains
G – geometric extinction cross-section
$Q_{\rm ext}$(composition, size, λ) – extinction efficiency factor
$n_{\rm d}$ number density of dust grains
D – distance to the star

Spherical particles:

$$A(\lambda) = 1.086\,\pi r_{\rm s}^2\,Q_{\rm ext}(m, r_{\rm s}, \lambda)\,n_{\rm d}\,D$$

$m(\lambda) = n(\lambda) + k(\lambda)\,i$ – complex refractive index
$r_{\rm s}$ – particle radius

UV extinction: small particles in the ISM

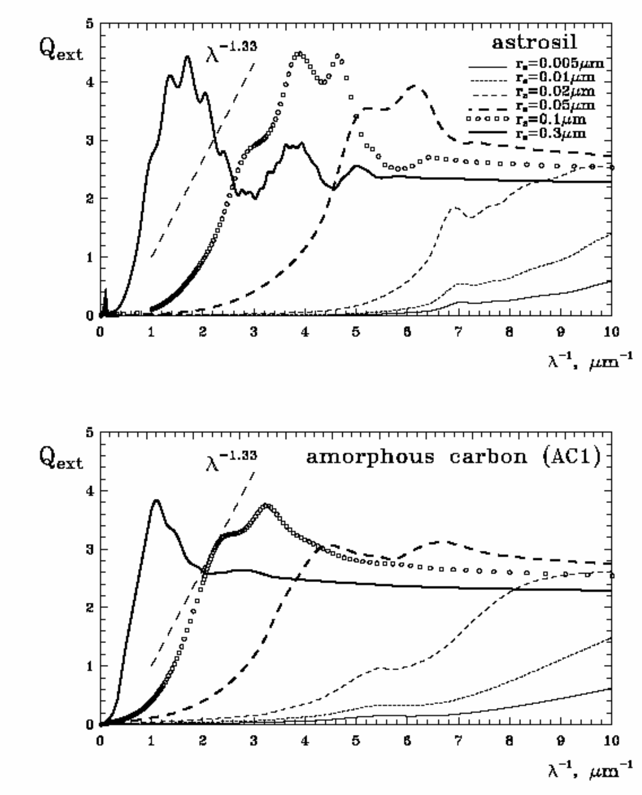

Figure 24 Wavelength dependence of the extinction efficiency factors for homogeneous spherical particles of different sizes consisting of astronomical silicate and amorphous carbon. The dashed segment shows the approximate wavelength dependence of the mean galactic extinction curve at optical wavelengths.

Bump 2200 A – small graphite particles

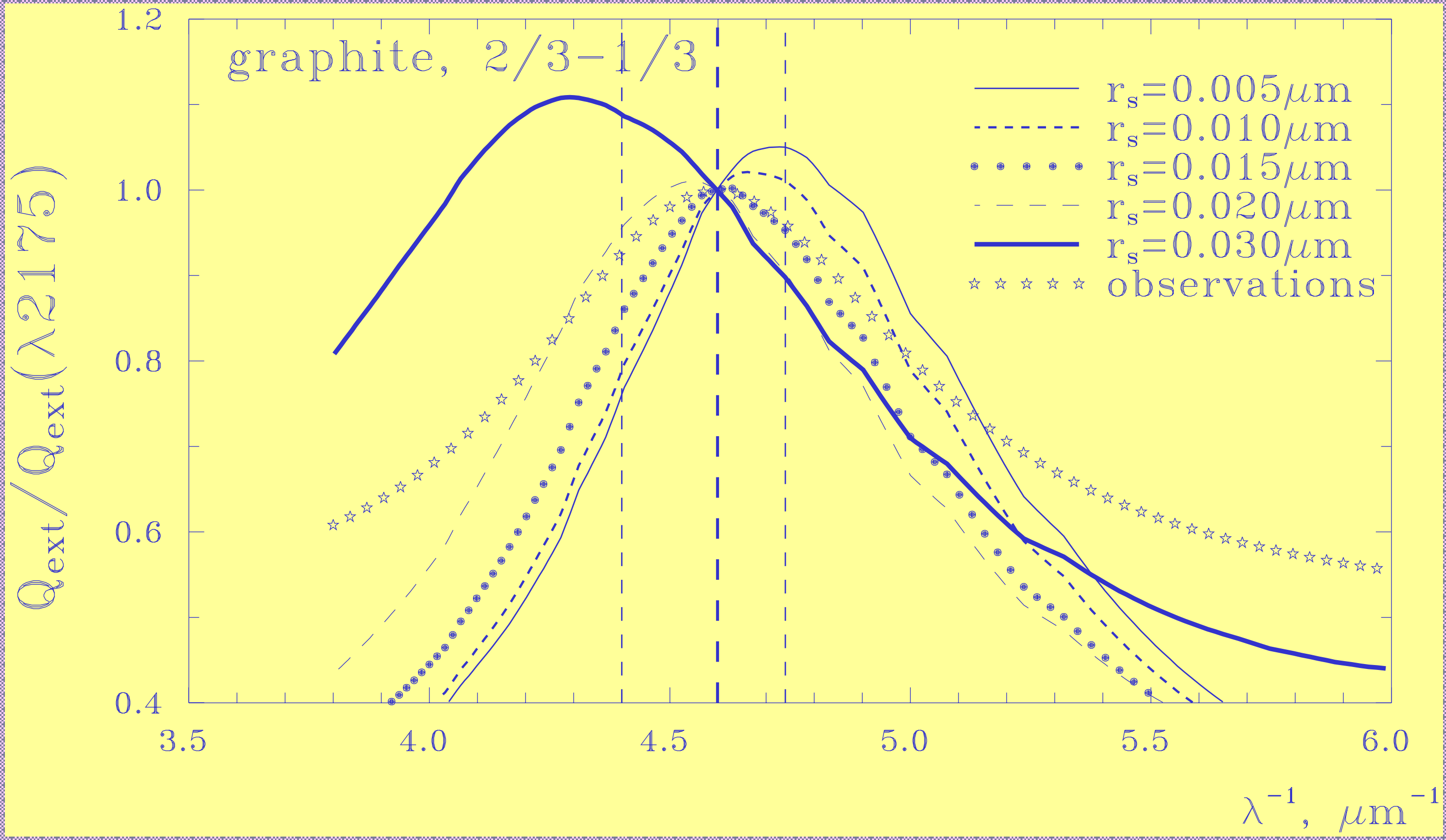

Interplanetary dust grains
(NASA collection)

L2021A1

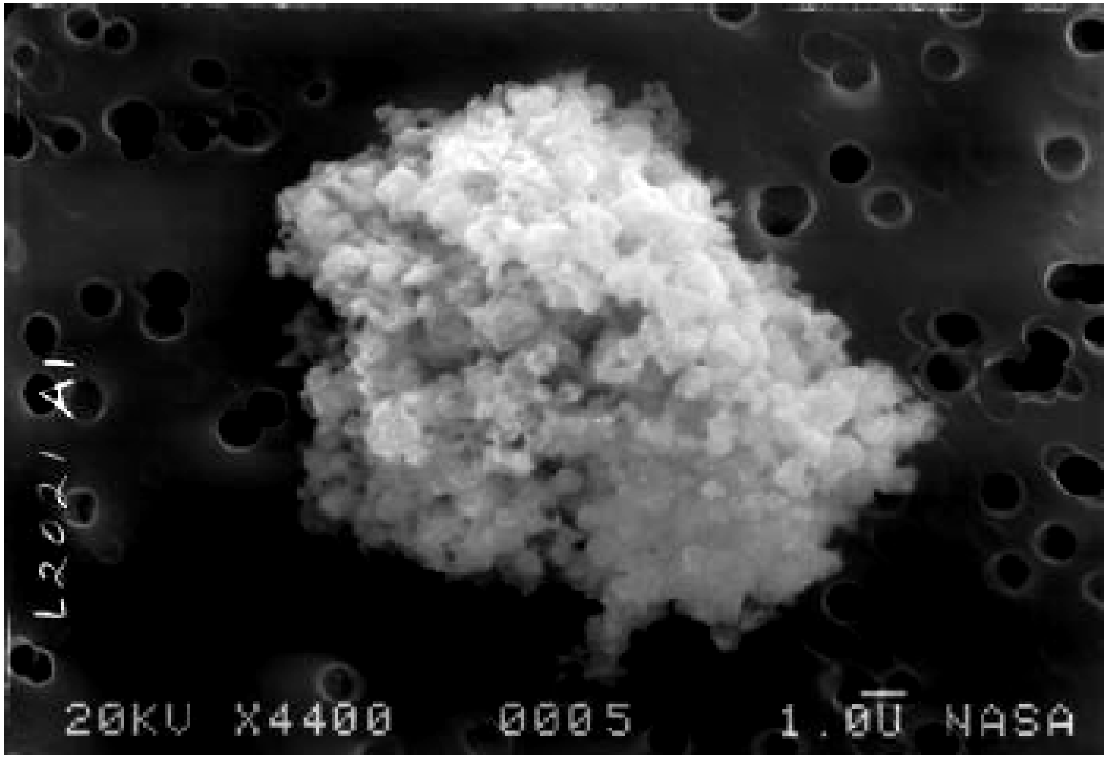

97E00328

Size:	16
Shape:	I
Trans:	TL
Color:	Black-White
Luster:	D
Type:	C
Comments:	Cluster 1

Cometary's (?) grains

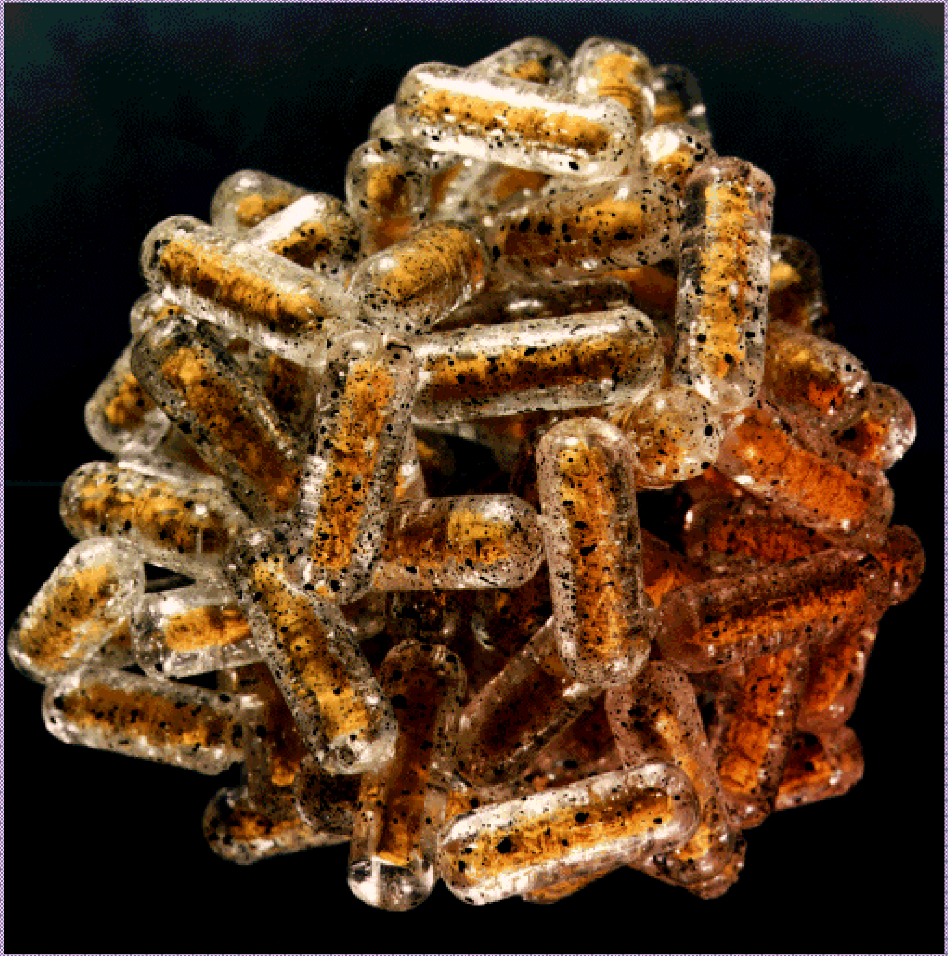

Interstellar (?) grains

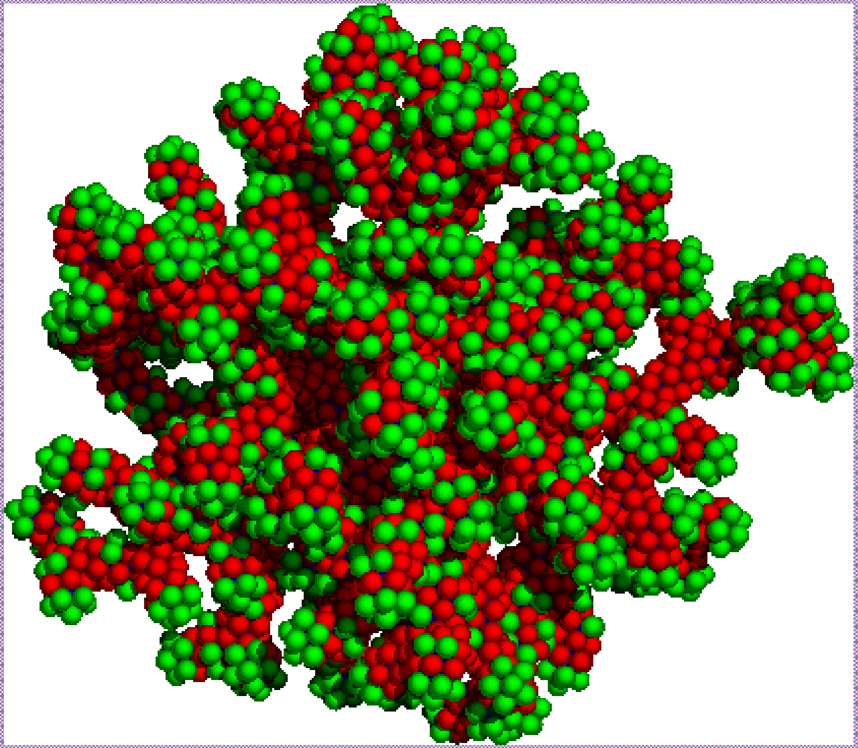

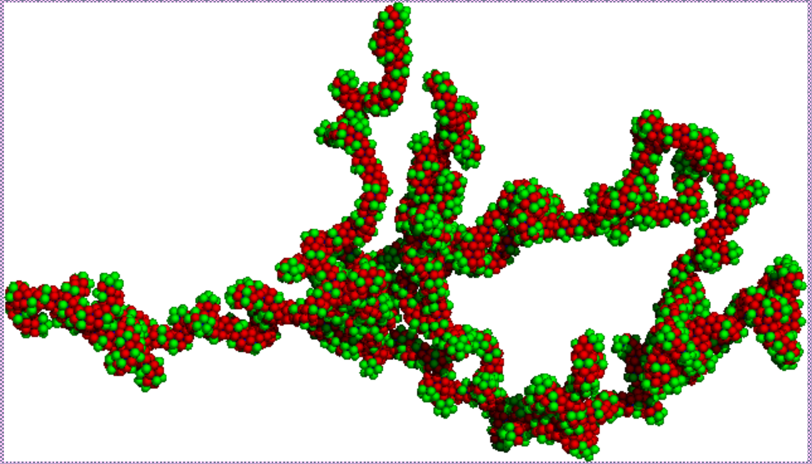

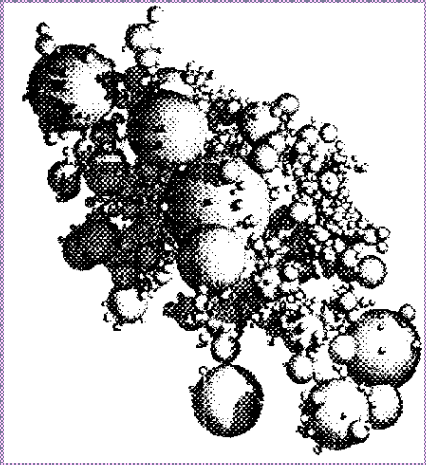

Absolute extinction and abundances

$$\left[\frac{X}{H}\right]_{\rm d} = \frac{A_{\rm V}}{1.086 N({\rm H})} \left[\frac{C_{\rm ext}(\lambda_{\rm V})}{V}\right]^{-1} \sum_i \frac{\rho_i}{m_i} n_i^X \frac{V_i}{V}$$

$$= 1.228 \cdot 10^6 \, R_{\rm V} \left[\frac{N({\rm H})}{E({\rm B}-{\rm V})}\right]^{-1} \frac{r_{\rm s}}{Q_{\rm ext}(\lambda_{\rm V})} \sum_i \frac{\rho_i}{m_i} n_i^X \frac{V_i}{V}.$$

- observed quantities: interstellar extinction $A_{\rm V}$ and hydrogen column density $N({\rm H})$;
- model parameters: mass of constituents in a grain m_i, the relative part of the element X in the constituent i, n_i^X, density of grain material ρ_i and relative volume of the constituent in a particle V_i/V and
- a calculated quantity: the ratio of the extinction cross-section to the particle volume $C_{\rm ext}/V$.

Problem ???

How to model extinction,… taking into account dust-phase abundances, inhomogeneous particle structure,…???

Three approaches to the modelling

1. Two or more populations of compact particles

Calculations: Mie theory

2. Mixing of materials

3. consisting of different materials in the form of inclusions (or layers)

Calculations: DDA (nMie)

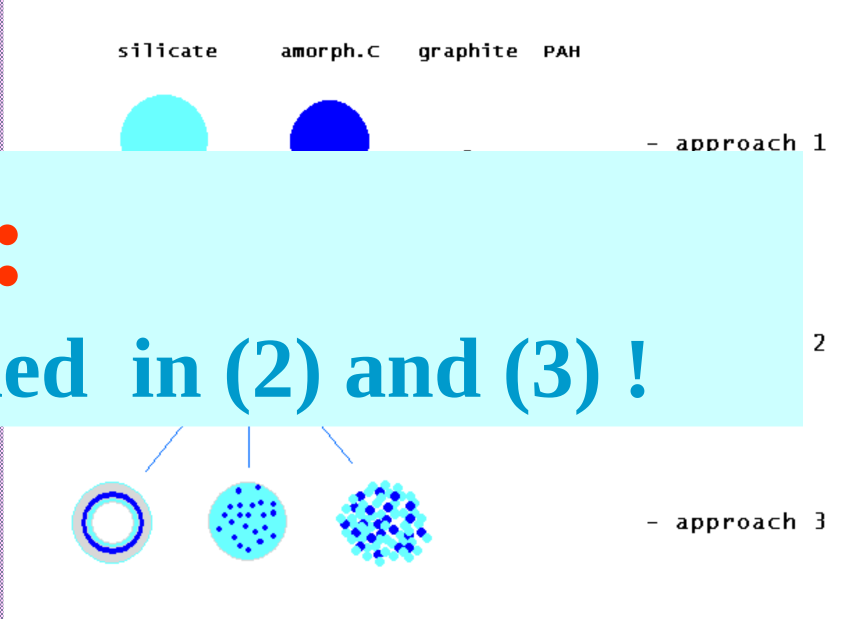

IMPORTANT:

Vacuum can be included in (2) and (3) !

DDA vs layered spheres

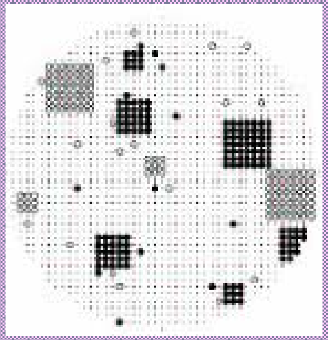

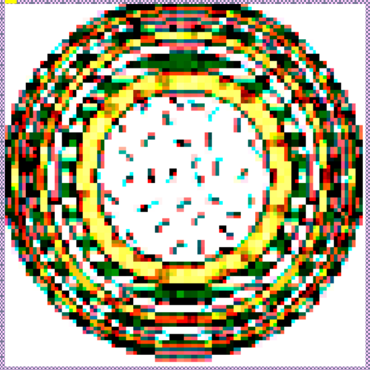

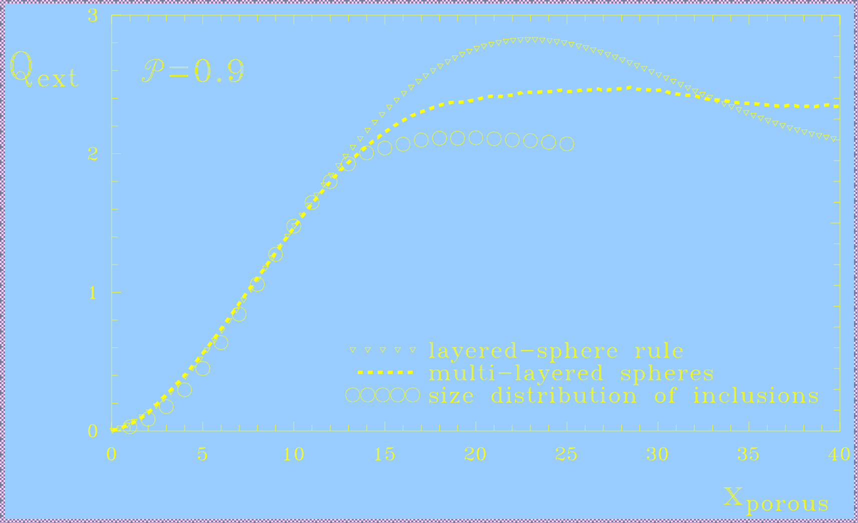

Interstellar extinction:
normalized cross sections

$$C^{(\mathrm{n})} = \frac{C(\text{porous grain})}{C(\text{compact grain of same mass})} = (1-\mathcal{P})^{-2/3}\,\frac{Q(\text{porous grain})}{Q(\text{compact grain of same mass})}.$$

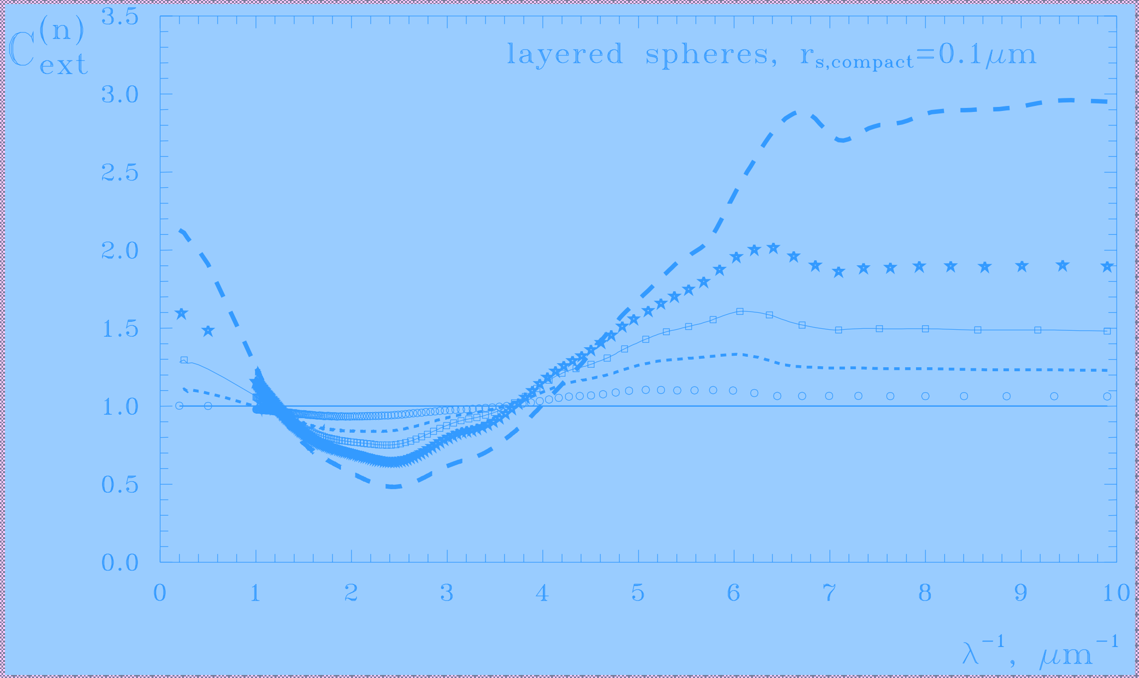

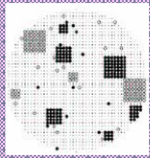

Modelling: extinction (zeta Oph) + dust-phase abundances (single size dust particles)

Oxygen abundance (homogeneous sphere)
O/H, ppm (dust)
astrosil (MgFeSiO$_4$)
amorphous forsterite (Mg$_2$SiO$_4$)
ζ Oph
300
250
200
150
100
0.0
0.5

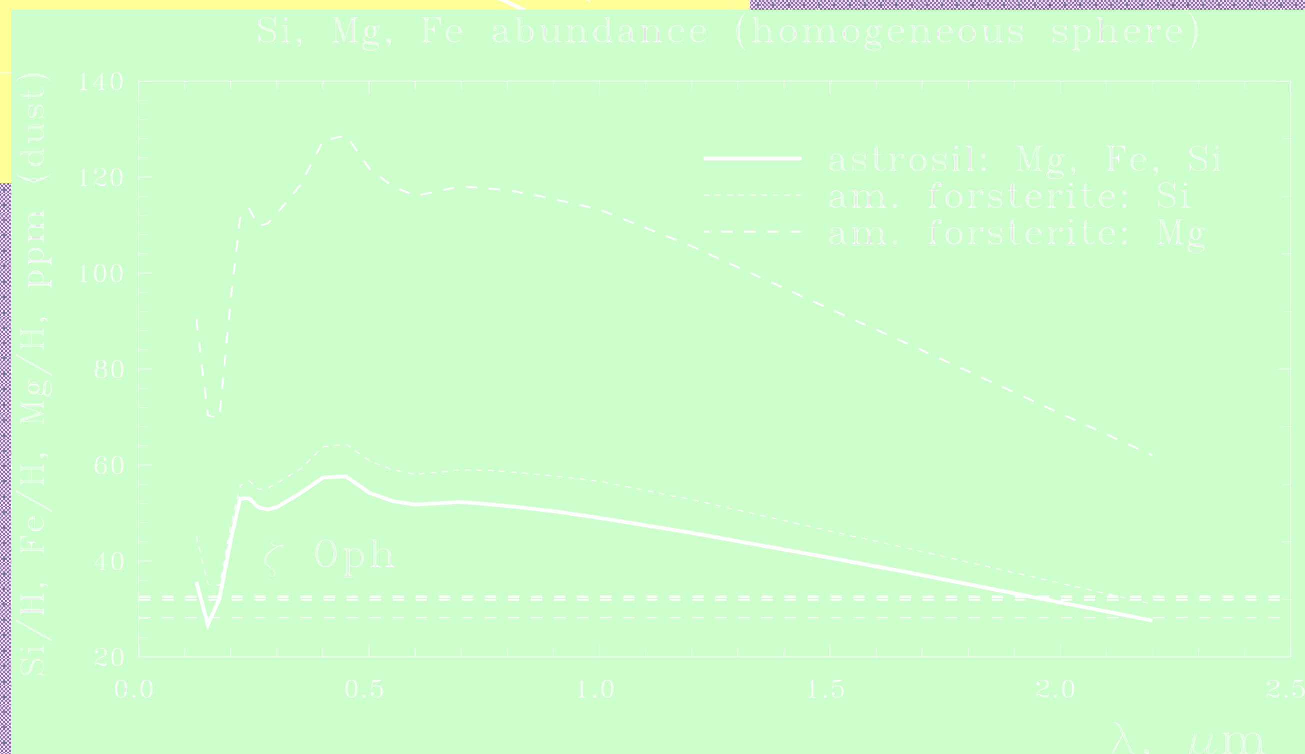
Si, Mg, Fe abundance (homogeneous sphere)
Si/H, Fe/H, Mg/H, ppm (dust)
astrosil: Mg, Fe, Si
am. forsterite: Si
am. forsterite: Mg
ζ Oph
140
120
100
80
60
40
20
0.0
0.5
1.0
1.5
2.0
2.5
λ, μm

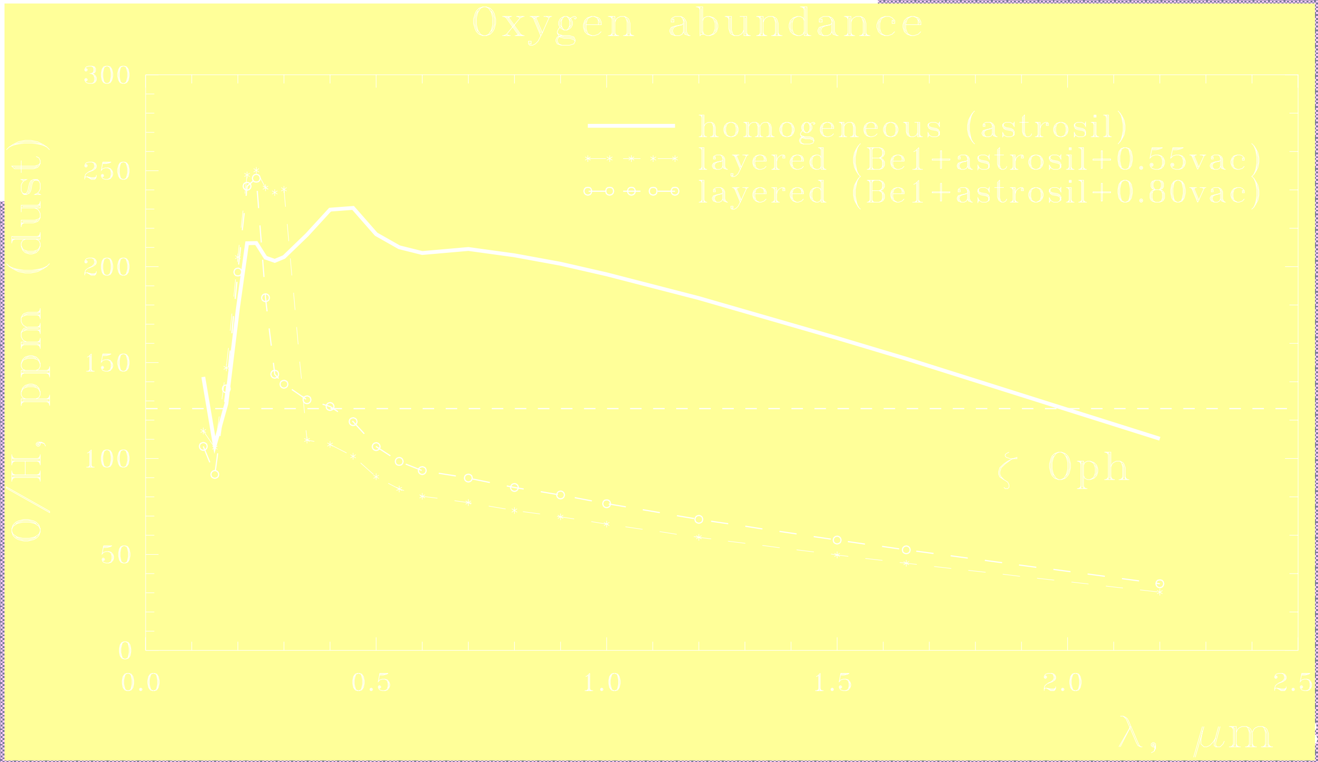
Oxygen abundance
homogeneous (astrosil)
layered (Be1+astrosil+0.55vac)
layered (Be1+astrosil+0.80vac)
ζ Oph
O/H, ppm (dust)
λ, μm
0.0
0.5
1.0
1.5
2.0
2.5
0
50
100
150
200
250
300

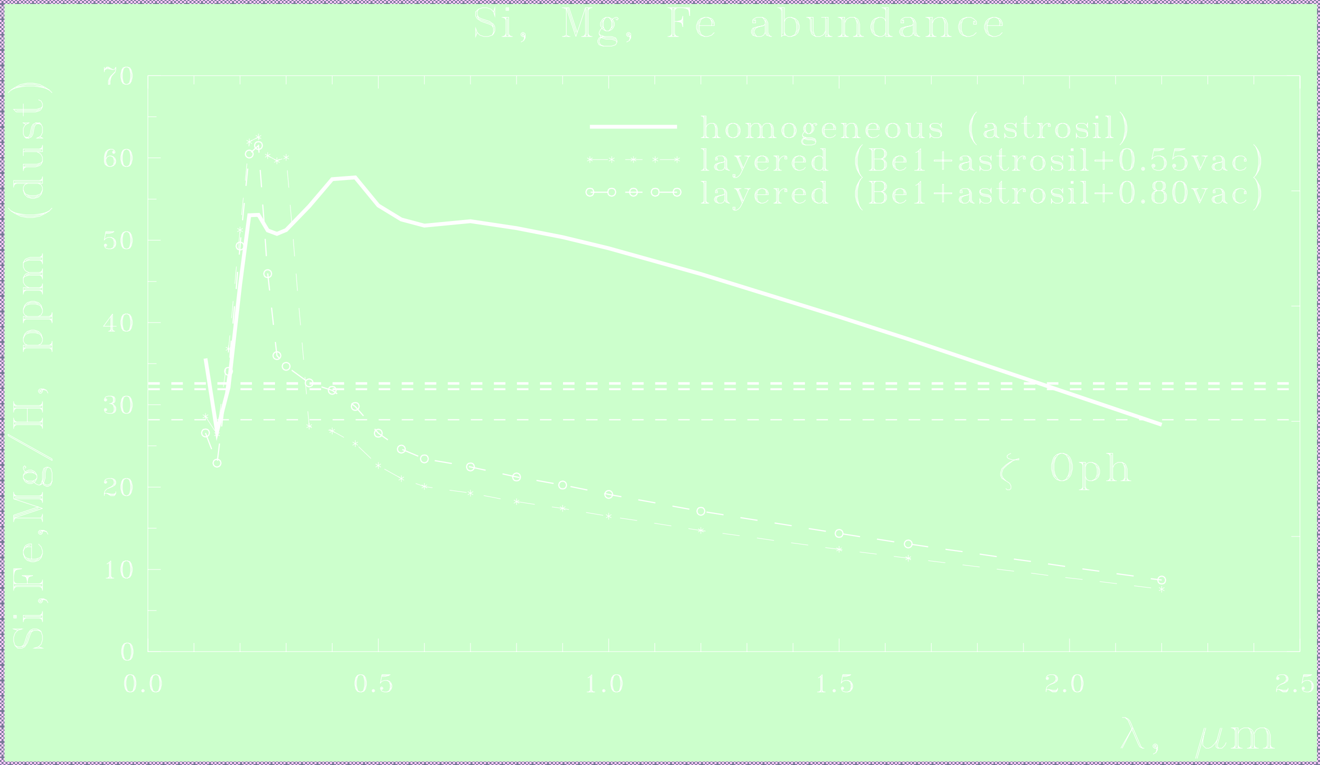
Si, Mg, Fe abundance
Si,Fe,Mg/H, ppm (dust)
homogeneous (astrosil)
layered (Be1+astrosil+0.55vac)
layered (Be1+astrosil+0.80vac)
ζ Oph
λ, μm
0.0
0.5
1.0
1.5
2.0
2.5
0
10
20
30
40
50
60
70

Interstellar extinction and abundances

Voshchinnikov et al., Astron. Astrophys., 445, 167, 2006;

zeta Oph (HD 149757)

Av = 0.94 mag.

	obs	model
C	110	219 ppm
O	126	124
Mg	32	22.7
Si	33	28.2
Fe	28	36.1

(I) & (III) - very porous particles

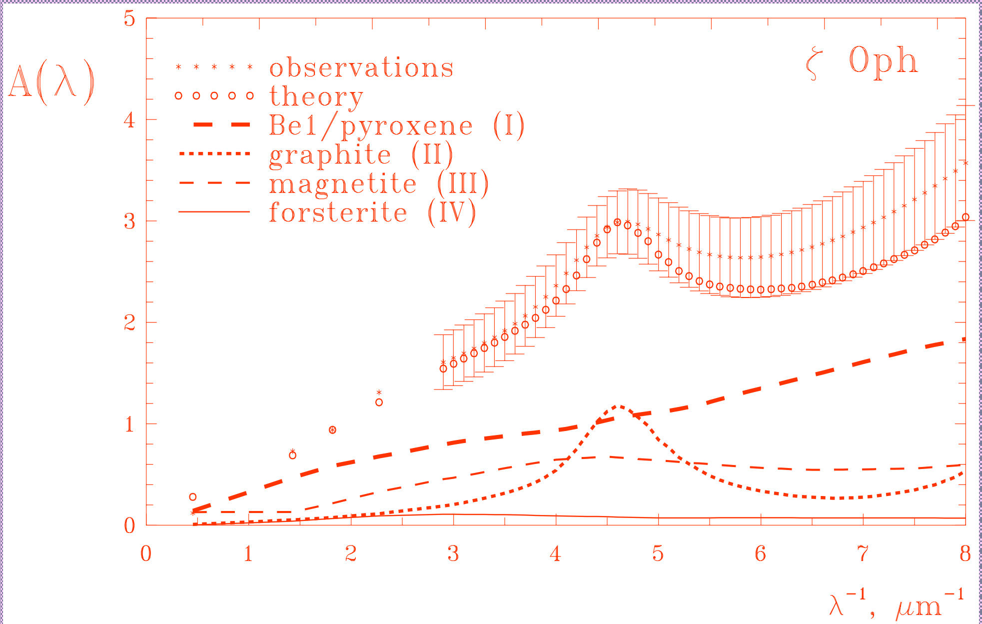

Interstellar extinction and abundances

Voshchinnikov et al., Astron. Astrophys., 445, 167, 2006;

sigma Sco (HD 147165)

(I) & (III) - very porous particles

A_V = 1.13 mag.

	obs	model
C	176	137 ppm
O	85	71
Mg	30.9	17.7
Si	32.4	8.8
Fe	27.9	26.6

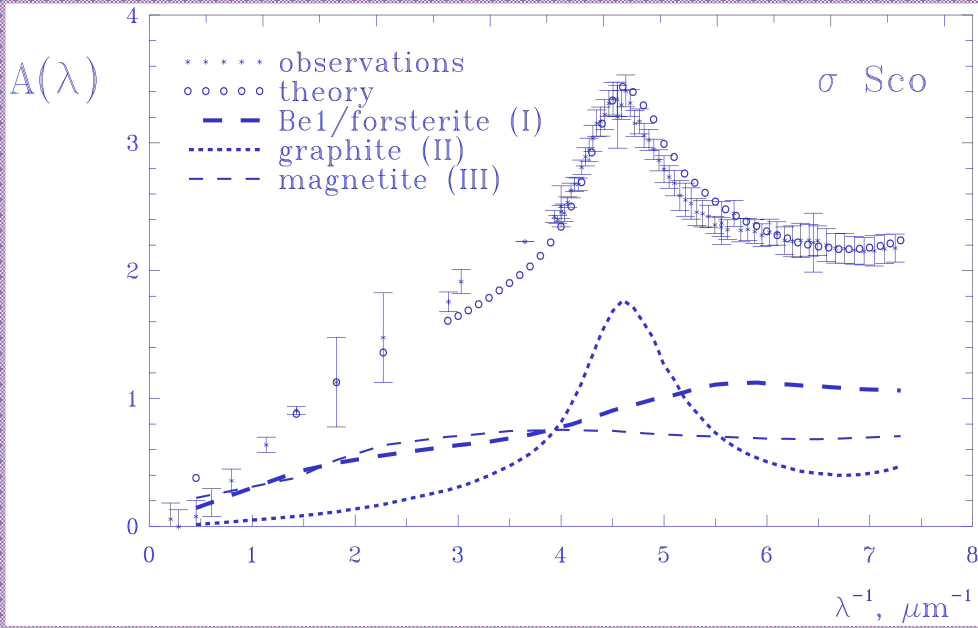

Some conclusions

- ***It is possible to model IS extinction taking into account dust-phase abundances***

Some conclusions

- **Cosmic abundances:**
- **solar ? ---- YES (local ISM)**
- **> solar (old solar) ? --- may be (large**
- **distances)**

X-ray abundances

(поглощение рентгеновского излучения связанными электронами с K- и L-оболочек – можно разделить газ и пыль!)

	new solar (2004)	Cyg X-1 71/+3/2kpc	Cyg X-2 87/-11/13kpc	4U1820-30 3/-8/8kpc
C	245			
O	457	492	478	485
Mg	33.9	59?		
Si	34.2	37?		
Fe	28.2	16.5	24.3	18.9

- ВСЁ!
- THANKS!

Cartledge et al. ApJ 641, 327, 2006 (STIS)

Газ + пыль

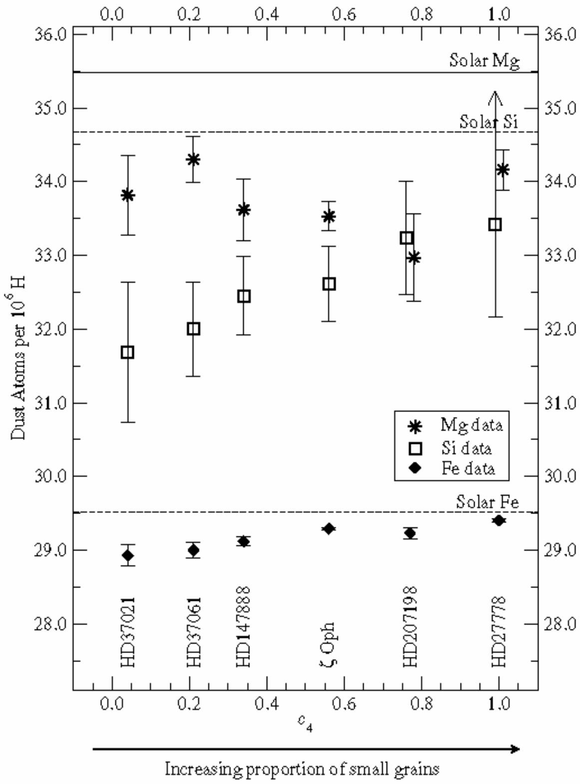

Fig. 10. Magnesium, silicon, and iron dust abundance variations with extinction curve parameter c_4 (Fitzpatrick & Massa 1990; Valencic et al. 2004). This plot combines Miller et al. (2005) iron and silicon results with magnesium data for translucent sight lines in the current sample; the points representing Si and Mg toward HD27778 and HD207198 are offset for clarity. The trend for both iron and silicon is an increasing dust abundance with c_4, a property that rises as small grains make up a larger fraction of the dust population. In contrast, magnesium abundances are relatively constant, or appear to decrease if HD27778 is neglected. HD27778 is unique among these paths for its very low nickel and carbon gas-phase abundances (§ 3.2; Sofia et al. 2004). Lodders (2003) photospheric abundances were adopted as the cosmic standard; Savage, Cardelli, & Sofia (1992) provided the ζOph data, which were adjusted to reflect currently-accepted f-values.

Fitting (подгонка)

$(1150\,\text{Å} \le \lambda < 2700\,\text{Å})$

$(y \equiv \lambda^{-1})$

$$A^{(n)}(y) = \frac{E(\lambda - \mathrm{V})}{E(\mathrm{B} - \mathrm{V})} = c_1 + c_2 y + c_3 D(y, W, y_0) + c_4 \tilde{F}(y),$$

where

$$c_2 = -0.824 + 4.717 \times R_{\mathrm{V}}^{-1},$$

$$c_1 = 2.030 - 3.007 \times c_2,$$

$$D(y, W, y_0) = \frac{y^2}{(y^2 - y_0^2)^2 + y^2 W^2}$$

and

$$\begin{cases} \tilde{F}(y) = 0.5392(y - 5.9)^2 + 0.05644(y - 5.9)^3, & \\ & \text{for } y \ge 5.9\,\mu\mathrm{m}^{-1}, \\ \tilde{F}(y) = 0, & \text{for } y < 5.9\,\mu\mathrm{m}^{-1}. \end{cases}$$

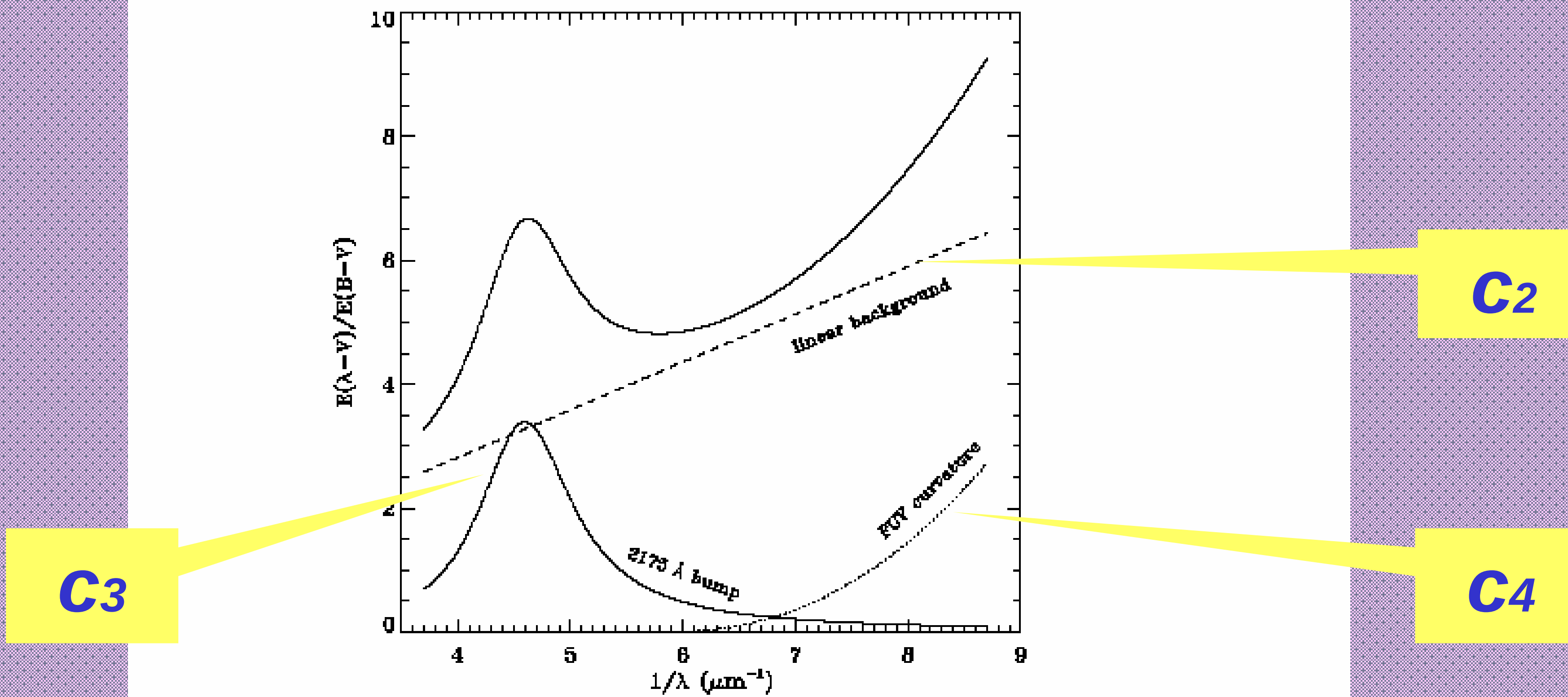

Figure 16 Analytical fitting functions for UV extinction curves from Fitzpatrick and Massa (1990). A normalized UV extinction curve (thick solid curve) can be represented by a combination of three functions: *i*) a linear background component (thin dashed line), *ii*) a UV bump component (thin solid curve), and *iii*) a far-UV curvature component (thin dotted line). Parameterized functions are given by Eqs. (3.10)–(3.14). After Fitzpatrick (1999).

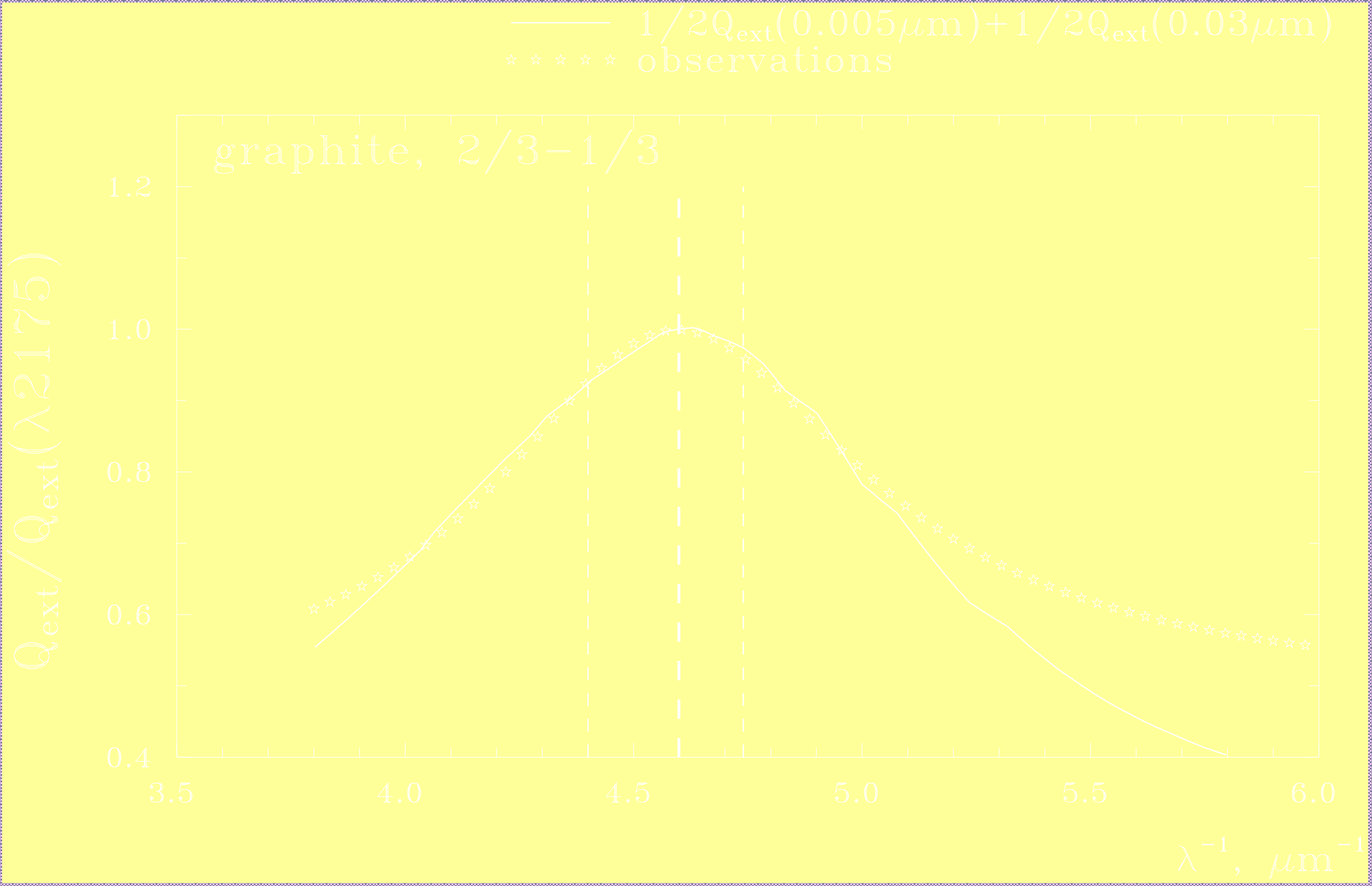

1/2Q$_{ext}$(0.005μm)+1/2Q$_{ext}$(0.03μm)
observations
graphite, 2/3–1/3
$Q_{ext}/Q_{ext}(\lambda 2175)$
1.2
1.0
0.8
0.6
0.4
3.5
4.0
4.5
5.0
5.5
6.0
λ^{-1}, μm^{-1}